MIGUEL JOSÉ SEABRA LOPES MACEDO FERREIRA

METHACRYLATED HYALURONIC ACID AND PECTIN CELL-LADEN HYDROGELS FOR SKIN EMULATION

Dissertação de Mestrado

Mestrado Integrado em Bioengenharia

Ramo de Biotecnologia Molecular

Universidade do Porto

2016

THIS WORK WAS SUPERVISED BY:

Dr. Pedro Lopes Granja

i3S - Instituto de Investigação e Inovação em Saúde da Universidade do Porto

Dr. Miguel Gama

CEB - Centre of Biological Engineering, Universidade do Minho

HOST INSTITUTION:

i3S - Instituto de Investigação e Inovação da Universidade do Porto

"The most dangerous thing you can do in life is play it safe."
Casey Neistat

ACKNOWLEDGEMENTS

This project was the final step of my five-year journey to complete my Master's degree in Bioengineering. During this period, several people gave their contribution to make it successful and to make me grow as a researcher and as a person.

I would first like to thank my supervisor, Dr. Pedro Granja, who has been crucial in shaping my academic career for the past three years. Thank you for the mentorship, availability and vision (and for not saying no to the craziest ideas).

I would also like to thank my co-supervisor, Dr. Miguel Gama, for all the support and guidance throughout the project.

To everyone in our team, particularly Filipa Sousa and Rúben Pereira, who helped me in experimental design and execution, for being there when I needed them, in the good times and the bad ones.

To all the technicians at i3S who provided me with training that allowed me to operate the equipment needed for my experimental work.

To the Achilles Team: Raquel, Daniel and Elsa for the crucial input and for being so helpful and supportive during the final days of writing and editing this document in Leiden.

And finally, to all my friends and family, particularly my parents Emília and José, sister Sofia and brother Nuno for all the vital support and effort to help me pave the way through this journey. I wouldn't be here if it wasn't for you.

ABSTRACT

The skin is an important component of the human body, having crucial defensive, immune and sensory roles. Even though its barrier properties confer vital protection against the external environment, they also pose a great challenge for drug delivery. Disruption of skin barrier often leads to the formation of acute or chronic wounds that affect millions of patients worldwide. Moreover, due to its great surface area and ease of access, there are numerous compounds that can have detrimental toxicological consequences for human health. All these factors contribute to a growing need to study and understand skin behaviour, not only from an academic perspective, but also with great implications for industry and governments worldwide. Novel scientific and technological breakthroughs are improving predictive accuracy of skin *in vitro* models, which resulted in some of them gaining international acceptance worldwide. However, these models are often simplified, do not account for skin complexity and work in a low-throughput manner. Recently, microfluidic devices have emerged as novel methodologies to emulate biological functions. However, only a few skin emulative microfluidic devices have been developed so far, which only allowed limited types of assays to be performed. Therefore, this work was focused on the development and characterization of a novel material based on methacrylated hyaluronic acid (HAMA) and methacrylated pectin (PectMA) that could be used to create an *in vitro* skin model compatible with a high-throughput skin microfluidic device. Material compositions with different HAMA/PectMA ratios and concentrations were evaluated envisioning the optimization of the system in terms of mechanical and biological performance. Increasing the concentration of HAMA or PectMA generated hydrogels with higher shear elastic moduli (G'). Indeed, mechanical performance was dependent on polymer ratios. When cultured with dermal fibroblasts, gels with 0.75% HAMA did not keep their integrity for the 7 days in culture, requiring the addition of a low PectMA concentration (0.125%). Mixed hydrogels with 0.75% HAMA / 0.125% PectMA appeared to promote cell clustering and a more elongated morphology than the remaining formulations. Polymer modification with cell-adhesive RGD peptides had a notable influence in cell behaviour, promoting cell spreading and leading to hydrogel disk contraction and the production of endogenous extracellular matrix, evidenced by the formation of a fibronectin network that was denser in hydrogels fabricated with higher RGD content. Together, these results suggest that soft hydrogel systems composed of HAMA and PectMA may become useful for the creation of *in vitro* skin models for skin organ-on-a-chip applications.

RESUMO

A pele é um componente importante do corpo humano, desempenhando papéis cruciais a nível de defesa, imunitário e sensitivo. Apesar das suas propriedades de atuar como barreira conferirem proteção vital contra o ambiente externo, estas também se tornam num grande desafio para entrega de fármacos. A dirupção da barreira da pele leva por vezes à formação de feridas agudas ou graves que afetam milhões de pacientes mundialmente. Além disso, e devido à sua grande área de superfície e facilidade de acesso, existem vários compostos que podem levar a consequências tóxicas negativas para a saúde humana. Todos estes fatores contribuem para uma necessidade crescente de estudar e compreender o comportamento da pele, não apenas numa perspetiva académica, mas também a nível industrial e governamental. Recentes descobertas científicas e tecnológicas têm aumentado o poder preditivo de modelos de pele *in vitro*, resultando em alguns deles terem ganho aceitação internacional. No entanto, estes modelos são muitas vezes simplistas, não têm em conta a complexidade da pele e funcionam numa forma *low-throughput*. Recentemente, dispositivos de microfluídica têm surgido como novas metodologias para emular funções biológicas. No entanto, apenas alguns dispositivos deste género foram desenvolvidos para a pele, permitindo apenas a execução de um número limitado de ensaios. Assim, este trabalho foi focado no desenvolvimento e caracterização de um novo material baseado em ácido hialurónico metacrilado (HAMA) e pectina metacrilada (PectMA) que poderá ser usado para criar um modelo de pele *in vitro* compatível com um modelo de microfluidica *high-throughput*. Composições de materiais com diferentes rácios e concentrações de HAMA e PectMA foram avaliados com o intuito de otimizar o sistema a nível de propriedades mecânicas e biológicas. Aumentando a concentração de HAMA ou PectMA foi possível criar hidrogéis com maior módulo, mostrando uma dependência das propriedades mecânicas dos rácios poliméricos. Quando em cultura com fibroblastods da derme, géis com 0.75% HAMA não mantiveram a sua integridade durante os 7 dias em cultura, requerendo a adição de baixas concentrações de PectMA (0.125%). Hidrogéis mistos compostos por 0.75% HAMA / 0.125% PectMA promoveram *clustering* celular e uma morfologia mais alongada do que as restantes formulações estudadas. Modificação dos polímeros com péptidos RGD que permitem adesão celular teve uma influência notável no comportamento celular, promovendo *spreading* celular e levando a uma contração dos discos e produção de matrix extracelular endógena, evidenciada pela formação de uma rede de fibronectina, mais densa em hidrogéis fabricados com maior conteúdo de RGD. Assim, estes

resultados sugerem que hidrogéis macios compostos por HAMA e PectMA podem vir a ser úteis para a criação de modelos de pele *in vitro* para aplicações *organ-on-a-chip.*

TABLE OF CONTENTS

LIST OF FIGURES

LIST OF TABLES

LIST OF ABBREVIATIONS

2D: Bidimensional

2H2O: Deuterium oxide

3D: Tridimensional

ATR-FTIR: attenuated total reflectance-Fourier transform infrared

BSA: bovine serum albumin

DAPI: 4',6-diamino-2-phenylindole dihydrochloride

DMEM: Dulbecco's Modified Eagle Medium

ECM: extracellular matrix

EGF: Epidermal growth factor;

FBS: Fetal Bovine Serum

FT: full-thickness

HA: Hyaluronic acid

HAMA: methacrylated hyaluronic acid

HDNF: Human dermal neonatal fibroblasts

HSE: Human skin equivalent;

HSE: human skin equivalents

Irgacure 2959: 2-Hydroxy-4'-(2-hydroxyethoxy)-2-methylpropiophenone

KC: Keratinocyte culture;

LD50: dermal Lethal Dose, 50%

LM: Low-methoxyl

MA: Methacrylic anhydride

MMPs: matrix metalloproteases

MOC: Multi-Organ-Chip

MTT: 3-(4,5-dimethylthiazol-2yl)-2,5-diphenyl tetrazolium bromide

NaCl: Sodium chloride

NaOH: Sodium Hidroxyde

NMR: Nuclear magnetic resonance

OECD: Organization for Economic Co-operation and Development

PBS: phosphate buffered saline

PDMS: polydimethylsiloxane

PectMA: Methacrylated Pectin

PTFE: Polytetrafluoroethylene

RGD: Arg-Gly-Asp

RHE: reconstructed human epidermis

SB: Skin biopsy

SC: Stratum corneum

SEM: standard error mean

T2O: Tritiated water

TBS: tris-buffered saline solution

TER: transcutaneous electrical resistance

TEWL: Transepidermal water loss

UV:Ultraviolet

CHAPTER 1: INTRODUCTION

The human skin is a vital agent playing important roles not only as a mechanical and chemical defence mechanism, but also as a relevant immune and sensory organ [1]. It is composed of three main layers: epidermis, dermis and hypodermis where multiple interactions take place between different cell types and structures [2]. Its singular properties give it a paramount barrier role, protecting the human body against external agents and preventing water loss [3]. However, even though its barrier properties are crucial for homeostasis, they pose a great challenge for drug delivery. Due to its easy accessibility and the fact that it allows to circumvent hepatic first-pass metabolism using relatively painless delivery systems, the skin has emerged as an important route for compound administration [4–6]. Therefore, strategies to overcome its barrier are now being the focus of multiple research efforts that often lead to the development of novel permeability enhancers that must not only be effective in overcoming the barrier but also safe to use [7].

On the other hand, skin barrier disruption can lead to the generation of acute or chronic wounds that have a great social and economic impact on the lives of millions of patients [8], making the discovery of new strategies towards improving wound repair and regeneration of paramount importance. There is a wide range of chemical substances and mixtures that can have detrimental toxicological consequences for human health through skin contact, thus requiring specific regulation and guidelines for their safety evaluation [9]. Advances in cell and tissue culture and engineering made possible to develop reliable *in vitro* methods to assess the behaviour of chemicals in contact with the skin [10–13]. The combination of cells, scaffolds and growth factors has led to the development of tissue engineered skin substitutes and novel advanced biomanufacturing strategies are now paving the way to the creation of more complex and biomimetic solutions [14]. Furthermore, due to their improved capacity to mimic biological systems, these methods are emerging as alternatives to *in vivo* animal studies, which are expensive and often fail to predict clinical results [15]. Even though simple *in vitro* cell culture studies are able to yield valuable information, more sophisticated systems are often required to model certain functions or properties [16]. In order for these systems to gain regulatory acceptance they should closely resemble *in vivo* skin behaviour, use standardized methodologies, and give reproducible and predictive results [17]. Internationally accepted methods are important and should be taken into consideration while developing novel model systems as these are accepted by academia, industry and governments for different applications such as classification and labelling of chemicals [9] and the testing of novel cosmetic products and formulations [18]. In the present chapter, the state-of-the-art of

current *in vitro* systems for transdermal transport, wound repair and cutaneous toxicity emulation will be revised, taking into consideration their compliance with international testing guidelines and current research needs. Advanced technologies, such as organ-on-a-chip models for skin applications, will be considered both in terms of their current features and upcoming potential to model skin functions and properties.

1.1. IN VITRO ASSAYS FOR DRUG DELIVERY STUDIES

Drugs or compounds can enter the human body through different routes. Overcoming the skin barrier is one of them as transdermal transport is usually painless, noninvasive [4] and avoids hepatic first-pass metabolism [5]. This makes it a valuable solution for drug delivery [19] and the study of cosmetics [20].

When a substance contacts the skin, its fate is determined by phenomena such as diffusion, partitioning, metabolism, phase changes, adsorption and absorption [21] that, all together, originate distinct contributions to its behaviour in the human body. The effects of these processes, not only individually but also combined, and their interactions throughout the different skin layers, are not trivial to assess or simulate and, despite notorious developments in *in silico* modelling systems [22], *in vitro* and *in vivo* assays are still crucial to understand the behaviour and assess the safety of novel compounds and formulations in contact with the skin, as noted by worldwide accepted recommendations from the Organization for Economic Co-operation and Development (OECD) [13,23]. *In vivo* models were the first to be established, having the advantage of providing information about the systemic behaviour of the substances, both in terms of kinetics and metabolism. However, they require the use of animals and radio-labelled compounds [24–26] and make the study of early absorption processes often difficult. Moreover, as animal skin has usually higher permeability than human, *in vivo* animal studies often overestimate percutaneous absorption [24].

In order to develop accurate and reliable *in vitro* transdermal transport models, it is first necessary to understand what happens to a compound when it contacts the skin and as it moves through the different skin layers, as well as how this process can be influenced by different skin properties. Then, it is necessary to understand how skin permeability can be modulated. Although passive diffusion through the skin is important for delivery of some drugs, the enhancement of transdermal transport by disruption of the skin barrier function has been gaining interest in the last decades [6].

It has long been known that the top layer of the epidermis, the *stratum corneum* (SC), is the most important barrier to transdermal transport [27]. SC is composed of terminally

differentiated epidermal keratinocytes [28] and is characterized by having a “bricks and mortar” structure [29], with keratin-rich corneocytes acting as “bricks” embedded in extracellular hydrophobic “mortar” [30]. SC cell membranes have a higher lipid content compared to the whole tissue [31] and intercellular spaces that are rich in structural lipids having a prominent role in water retention [32,33] and acting as an entry barrier for non-lipidic or high molecular weight compounds [30]. Thus, the inability to hold water is often considered an indicator of barrier function impairment and increased susceptibility to external agents [34]. Skin barrier function is influenced not only by internal factors such as ageing [35] and circadian rhythms that influence skin pH, temperature and transepidermal water loss (TEWL) throughout the day [36], but also via external factors that are known modulators of SC properties. Here, pH has an effect on structural integrity and barrier function recovery [37]; relative humidity interferes with the mechanical properties [38]; high temperature leads to lipidic structural disorder and decreased resistance to water flow [39]; compounds such as fatty acids have been shown to increase fluidity, enhancing drug flux [40]; and alpha hydroxyacids contribute to maintaining skin barrier function against irritation [34]. After SC removal, the viable epidermis becomes the rate-limiting step to diffusion [41], making it relevant to study not only the influence of the SC, but also of the remaining skin layers in transdermal transport.

Besides its diffusional barrier properties, skin also plays an important metabolic role. There are different enzymes which have metabolic relevance in human skin, contributing for Phase I and Phase II metabolism, as reviewed elsewhere [42,43]. The first-pass effect of the skin on topically applied compounds tends to be spatially confined and, in contrast with oral administration, is able to overcome hepatic enzyme reactions before entering circulation [43]. However, it is still important to consider metabolic effects when developing *in vitro* transdermal transport models as some compounds are modified while going through this barrier [44]. This can be accomplished with the use of viable tissue, with active biotransformation enzymes [44].

One of the most well-known non-invasive drug delivery strategies is the use of transdermal patches, which were first introduced in the 1970s [19]. Currently, these are usually active for a period from one to seven days, being applied to deliver compounds such as clonidine, estradiol, fentanyl, lidocaine, nicotine, nitroglycerine, scopolamine and testosterone for applications in cases of hypertension, birth control, hormone replacement, among others [19,45]. However, as skin poses a significant barrier to the transport of many compounds of interest, different methodologies to overcome this problem have been developed in the last decades [6]. Not only the use of strategies such as chemical enhancers [46] like fatty acids [40],

fatty alcohols [47], surfactants and microemulsions [48], but also more sophisticated techniques such as ultrasounds [49] and microneedles [50] have been shown to increase skin permeability. Moreover, combinations of different chemical enhancers [7] or enhancing techniques have been observed to act synergistically [51], making combinatorial screenings a promising approach for improving transdermal transport avoiding skin irritation [7].

1.1.1. In vitro transdermal transport and skin barrier function models

In vitro studies are crucial for primary evaluation of novel compounds or formulations that contact the skin. The OECD guidelines for testing chemical compounds recommend the use of diffusion cell assays to investigate transdermal transport. This type of setup consists in a human or another animal skin sample between a donor and a receptor chamber. The test substance is applied on the surface of the skin and left for a period of time, followed by appropriate removal. Evaluation of the substance or its metabolites can be performed in the receptor fluid, even though it is also important to consider the amount remaining absorbed in the skin [13]. Moreover, these assays can be performed in steady state, with an infinite dose or non-steady state, with finite doses. Even though it is possible to extract relevant information from steady-state assays, finite dose studies are usually closer to what happens during real human exposure [52].

In order to evaluate skin integrity prior to absorption studies [24] and to assess the effects of techniques that modulate skin permeability, *in vitro* model systems that are capable of a robust evaluation of *in vitro* skin barrier function are necessary. This property can be analyzed *in vitro* with techniques such as tritiated water flux [53], evaporimetry [53] and electrical resistance measurements [54]. Tritiated water (T_2O) flux measures skin permeability to radioactive water. T_2O is applied on the epidermis and travels across the skin, being collected and evaluated for radioactivity after barrier transposition [53]. On the other hand, evaporimetry has been applied to measure TEWL, an indicator of skin water-holding capacity [34,53]. However, as this process is not only dependent on water diffusion through the skin but also on its evaporation and partitioning at SC surface, factors such as environmental relative humidity, temperature or air flow may come into play [53,55]. Therefore, correlations between TEWL and measures of T_2O flux have been performed in some cases [53,56]. Finally, skin electrical resistance measurements have also been pointed out as alternatives to evaluate skin integrity *in vitro*. Resistance can be quantified by applying a fixed current between two electrodes across a skin sample. This is a safe and faster method that can be used with *in vitro* diffusion chambers [54].

Regarding the choice of skin source, viable human skin obtained from autopsies or cosmetic surgery is the current gold standard for transdermal transport studies [57]. Yet, its availability is limited and a high variability is usually observed between donors in terms of age, gender and race [58]. For *in vitro* assays, fresh [59] or previously frozen [53] samples can be used. However, even though the latter may be a more convenient option, the freezing and thawing process may lead to tissue necrosis [59]. Fresh and frozen human skin may show similar permeability coefficients to water absorption [60], but behave differently for permeation of other compounds [59]. Moreover, the freezing process may inactivate a number of biotransformation enzymes [59], while others stay active [61]. Therefore, and depending on the compound in study, the use of fresh skin may be recommended.

Contrary to skin from human subjects, animal skin presents higher availability and controllability control in terms of donor age and gender [58]. Some of the most commonly used animal skin sources are rodents [62,63], rabbits [25] or pigs [25,62–64]. Rat skin permeation rate and concentration have been reported to be of the same order of magnitude as human skin for some topically applied substances with a wide polarity range (salicylic acid, hydrocortisone, clotrimazole and terbinafine) [62] but higher permeation has also been verified for compounds such as hydrocortisone [62] and paraquat [63,65], among other substances. Nevertheless, after comparative percutaneous absorption *in vitro* studies using diffusion cell assays, pig skin has been considered the closest *in vitro* alternative to human skin [62,63] and it has shown better performance than rat skin in particular for permeability levels of lipophilic compounds [63].

Besides human and animal skin, it is also possible to evaluate transdermal transport using *in vitro* human skin equivalents (HSE) that can either be composed of SC and viable epidermis as reconstructed human epidermis (RHE) models, or include an additional dermal layer as full-thickness (FT) models [66]. This type of *in vitro* models exhibit reduced variability but tend to have enhanced permeability levels when compared to human or pig skin *ex vivo* [66]. Moreover, as this kind of constructs usually lack skin appendages such as hair follicles, they may not be suitable for studying transport phenomena such as follicular penetration [67].

1.1.1.1. Low-throughput models

Transdermal transport studies *in vitro* are usually performed with diffusion chambers. Franz Diffusion cells (Figure 1a) are static models that were introduced in 1975 as a way to replicate percutaneous absorption [68] and are now commercially available with a widespread use [41,69]. Their design consisted in skin samples placed over an O-ring ball joint separating two parts of a glass chamber. The epidermal side was exposed to air while a buffer solution was in

contact with the dermal portion. The dermal solution was under magnetic agitation and controlled temperature conditions and could be removed, replaced and analysed at different time points during the transdermal transport assays [68]. Even though this model was versatile, allowing infinite [70] and finite [68] dose studies, it did not allow a continuous perfusion of the sample and required large volumes of skin.

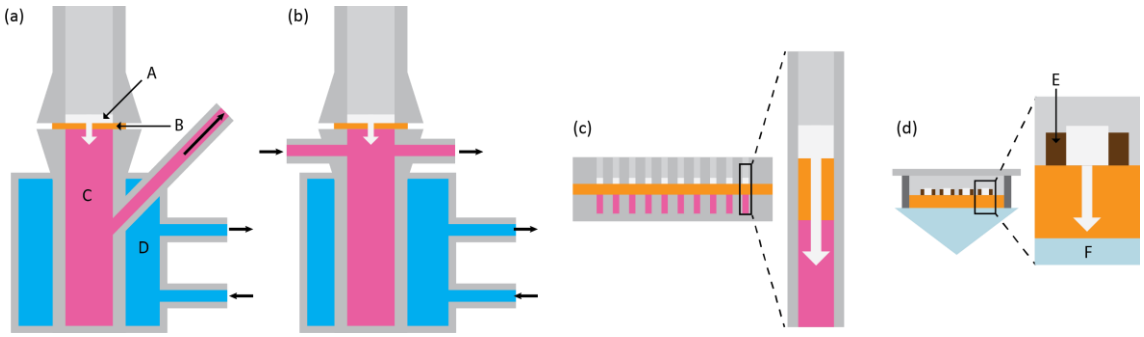

Figure 1: Transdermal transport models; (a) Franz diffusion cell; (b) Flow-through diffusion cell; (c) High-throughput transdermal transport model using plates with an array of orifices; (d) High-throughput transdermal transport model using paraffin to isolate different skin portions; Legend: A: test compound; B: skin sample; C: receptor fluid; D: temperature regulating fluid; E: paraffin; F: ATR-FTIR crystal.

Flow-through diffusion cells (Figure 1b) were then developed, using a perfused fluid under the skin surface flowing with a defined rate. Identically to blood flow, the receptor fluid was constantly renewed, which made this strategy more biologically relevant for the study of compounds with limited solubility and allowed automatic sample collection making it more convenient for constant monitoring [71].

1.1.1.2. High-throughput models

The wide range of potential skin permeability enhancement strategies that can be applied alone or in combination to study transdermal delivery of different compounds makes it necessary to transition from conventional models to novel high throughput strategies. Conventional methodologies such as Franz diffusion cells are not compatible with high throughput screening since they require large skin areas and time-consuming sample setup and manipulation [46]. A high throughput method for up to 100 assays was developed allowing a 50-times higher efficiency in skin usage when compared with a Franz diffusion cell (Figure 1c). The model was based on two plates fixed to each other using four screws. The plates were drilled with an array of 100 (10x10) 3 mm orifices that acted as wells separated by a skin sample placed with the SC facing the donor plate and dermal side exposed to phosphate buffered saline (PBS) solution in the receiving plate. For validation, skin permeability was

challenged with chemical enhancers and evaluated with conductivity measurements [46]. This model has since been successfully applied to screen for synergic combinations of 32 different chemical enhancers as more than 5,000 formulations [7]. Even though it has shown promising results, permeability assessment has not been automatized.

Another strategy has been applied to study multiple formulations simultaneously in the same skin sample, using a paraffin automatic dispenser that was able to draw 16 octagonal wells with 2.4 mm diameter on a skin sample (Figure 1d). These wells acted as impermeable barriers containing different solutions that were manually applied with a pipette. Samples were further analysed with attenuated total reflectance-Fourier transform infrared (ATR-FTIR) imaging to measure the permeation of 4-cyanophenol, making it possible to study the over-time permeation of this compound in 12 samples simultaneously [72].

High-throughput strategies often require miniaturization. However, even though they may lead to a higher time efficiency while using a smaller skin area per sample, they open new challenges due to changes in permeability as a consequence of the decreasing skin-compound contact area. It has been described that, while using an array of donor reservoirs of different radii, skin permeability to mannitol decreases with increasing contact area [73].

Despite the great advantages of both models discussed above there seems to be considerable room for improvement. They both require considerable manipulation and, as they perform several assays on a single skin sample, using these techniques further scale-down may lead to cross-contamination between different assays due to lateral compound diffusion within the sample.

1.2. IN VITRO ASSAYS FOR WOUND HEALING STUDIES

Skin wounds can be classified as acute or chronic. Acute wounds often follow an organized reparative process while chronic wounds are usually not able to restore most of their anatomic and functional features [74]. Wound healing is a complex process requiring the interplay of several different agents. This process is composed of three major phases: coagulation and inflammation, new tissue formation and tissue remodelling [75,76]. The coagulation and inflammation phase are first characterized by the formation of a fibrin plug. This structure is composed of platelets embedded in a matrix of fibrin and other proteins, promoting haemostasis and providing temporary wound closure [77], while acting as a scaffold for new tissue formation and being a reservoir of chemokines and growth factors [78]. These soluble compounds are released from the injured site and recruit circulating inflammatory cells such as neutrophils and monocytes in order to clear and remove tissue remnants from the wounded

area [77]. During the following phase, the formation of new tissue, keratinocytes migrate, proliferate and maturate over the disrupted dermis, contributing to the restoration of skin epithelial barrier function properties [76]. This process of wound re-epithelization is of great importance and its malfunction may lead to the generation of chronic wounds. Its regulation is achieved by a range of soluble factors and surface protein interactions [79] combined with physical stimuli, such as electric fields promptly generated after skin epithelial disruption and condition keratinocyte migration [80]. In addition, endothelial cells form new blood vessels by angiogenesis and some capillaries colonize the fibrin clot, giving rise, along with macrophages and fibroblasts, to granulation tissue rich in collagen type III. Finally, macrophages stimulate fibroblast differentiation into a myofibroblast cell type with contractile activity, promoting wound closure [76]. The last phase, tissue remodelling, is characterized by a decrease in cellular activity, apoptosis at the wound site and extracellular matrix (ECM) remodelling by secreted matrix metalloproteases (MMPs), degrading type III collagen that is then replaced by type I [76,81].

Since skin wounds result in a considerable societal burden and economic impact [8] research towards a better understanding of wound healing is of paramount importance to generate new strategies to enhance wound repair and regeneration.

1.2.1. In vitro wound healing models

1.2.1.1 Low-throughput models

Wound repair studies can be performed *in vitro* using bidimensional (2D) or tridimensional (3D) skin models. While 2D models, focused on simple aspects of wound repair, are often easier and simpler to be performed, more complex 3D models better mimic tissue microenvironment and allow the study of a wider range of phenomena [82,83]. Different assays have been developed allowing the study of chemical agents [83] or physical stimuli, such as the influence of electric fields [84] or shear stress [85].

A simple 2D model approach developed to emulate wound repair is the *in vitro* scratch test (Figure 2 a). This affordable strategy to evaluate cell migration consists on the creation of a "scratch" on a confluent cell monolayer, followed by observation of cell migration from the edges of the gap towards its centre, in a process mimicking wound closure. While using a very basic approach, it has allowed continuous monitoring of the samples with time-lapse microscopy as well as evaluation of single cell migration [83]. An alternative to mechanical wounding studies has been developed using barrier migration assays (Figure 2d) where, instead of disrupting a cell monolayer, a wound model was created through the use of a

physical barrier insert that did not allow cell colonization of a certain area. Once that barrier was removed, cells moved over an unaltered surface, making it possible to evaluate cell migration using microscopy techniques [86].

A different strategy relies in studying cell migration through a membrane. This has been done through the use of the Boyden chamber assay that was proposed in 1962 as a way to study leucocyte chemotaxis (Figure 2f). A device composed of two compartments separated by a filter membrane was loaded with a cell suspension in one side and a test solution on the other. After incubation and membrane removal from the chamber, it was possible to assess cell migration using microscopy techniques to observe the number of cells that went from one compartment to the other through the filter [87]. Modifications of this technique have since been used in skin wound repair studies to evaluate the effect of both chemotactic promoters [88] and inhibitors [89].

On the other hand, 3D wound models can be created using scalpels [82,90], skin meshers [90], freeze damage [91] and laser irradiation [92]. These models are able to emulate wound repair in a more *in vivo*-like environment, allowing for a more complex study of biological processes. For instance, after scalpel incisional or excisional wounding of HSE constructs, it was possible to transfer them to the top of a collagen gel where they were kept at the air-tissue interface, and to observe keratinocyte migration, restoration of epithelial integrity, wound closure and stratification [82]. However, most wounding strategies require extensive tissue manipulation [82,90,91]. One way to reduce the need for manipulation while reproducibly creating wounds is to use laser irradiation. With this strategy, it was possible to control the magnitude of the damage by varying the number of laser pulses applied, affecting the epidermis alone or in combination with the dermis, creating reliable model wounds [92].

1.2.1.2. HIGH-THROUGHPUT MODELS

High-throughput systems have been developed not only for assessment of cell migration on flat surfaces [93] but also through a membrane [94].

A variation of the *in vitro* scratch test has been used for high-throughput analysis in a 384-well plate (Figure 2b). Cell monolayers were disrupted by a manually operated 96 array of pins, resulting in wounds of similar morphology in different wells that could be evaluated using fluorescence microscopy and automated image analysis [93]. More recently, a miniaturized system with high scale-up potential was used to evaluate cell migration. This method applied a laminar flow of trypsin to generate a wound model, promoting cell detachment and creating a gap in a fibroblast monolayer (Figure 2c). This system allowed the creation of wounds models with well-defined shape and edges and the study of the influence of different compounds on

fibroblast migration using a phase-contrast microscope [95]. In addition, the development of an integrated system was achieved using laser pulses to create wound models in 96-well cell cultures (Figure 2e). This high-throughput system used an automated mechanism for wound generation and image capturing at different time points after wounding. Following image analysis, wound area could be determined and wound healing levels estimated over time, making it possible to evaluate the closure of irregular-shaped wounds with no need for sample fixation and in a fast, high-throughput manner [96].

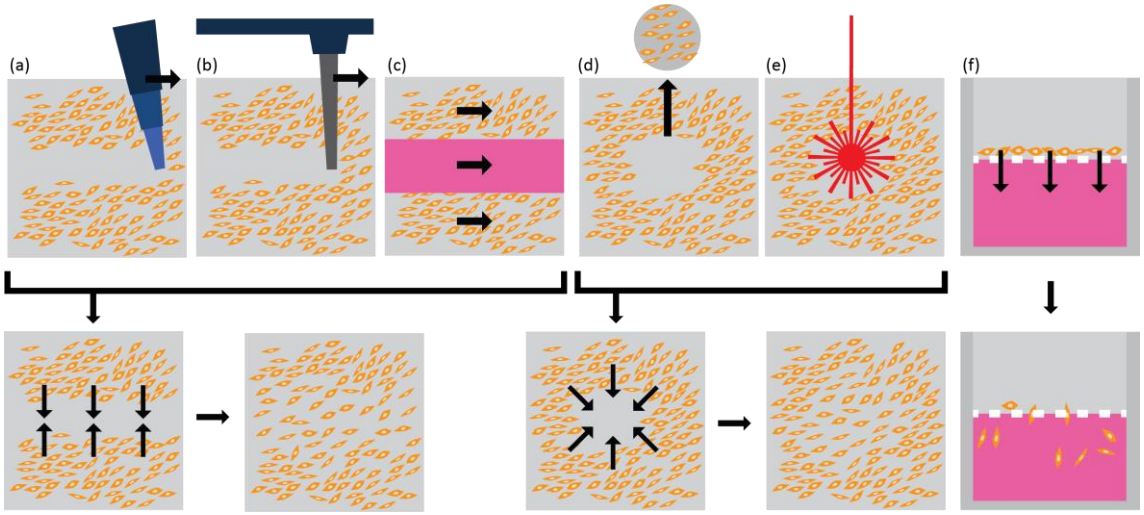

Figure 2: *In vitro* wound healing models. (a) *In vitro* scratch test using a micropipette tip; (b) *In vitro* scratch test using an array of pins; (c) wound model formation with a laminar flow of trypsin flanked by laminar flow of pbs; (d) barrier migration assay; (e) wound model formation with laser irradiation; (a-e): wounding and wound closure mechanisms. After wound formation, cells migrate towards the wounded area; (f) Boyden chamber assay.

Furthermore, a system using a modified Boyden chamber assay (Figure 2f) has also been applied to study cell migration and chemotaxis through a porous membrane in a 96-well format. By using a fluorescent staining of cell nuclei, the number of migrated cells was calculated through the use of an automated microscope and software analysis [94]. These novel methodologies, driven by advances in miniaturization, automation and image analysis are making it possible to create model systems that allow a simultaneous quantitative evaluation of multiple samples, contributing to advances in high-throughput screening of different potential wound repair modulators.

1.3. IN VITRO ASSAYS FOR SKIN TOXICITY STUDIES

Different substances and mixtures can have detrimental health consequences. Therefore, a classification and labelling system has been established by the United Nations. Health hazards

due to skin contact can be divided in toxicity, corrosion, irritation, and sensitization. It is possible to categorize substances or mixtures based on their acute toxicity using dermal Lethal Dose, 50% (LD_{50}) levels, which is the amount of a chemical necessary to kill 50% of a population of test animals. Skin corrosion and irritation are related to the generation of skin damage up to four hours after application of a test substance. Indeed, corrosion leads to irreversible damage, with visible necrosis in the epidermis and dermis, whereas irritation leads to reversible damage. A skin sensitizer is a substance that leads to an allergic response after contact with the skin. These classification systems are mainly based on animal studies and clinical information. However, other parameters such as pH and *in vitro* tests may also be considered in some cases [9], such as the ones recommended by the OECD for assessment of skin corrosion [12,97,98] and irritation [10]. Moreover, as the European Union Cosmetics Regulation has put a ban on animal testing and requires studies of the toxicological profile of the substances present in cosmetic products, studies related to skin irritation, sensitization and in some cases photo-induced toxicity are required for these cases [18]. Other studies such as genotoxicity can also become relevant [99] and the OECD has issued guidelines for its *in vitro* assessment [100].

Skin corrosion can be evaluated *in vitro* by measurements of transcutaneous electrical resistance (TER), a parameter that evaluates SC integrity and barrier function as recommended by OECD guidelines. After application of a test chemical on the surface of a skin disk placed inside a testing apparatus, TER should be evaluated after 24 hours and compared with standardized values. A corrosive effect is noticeable by a decrease of TER below a threshold level [97]. Even though this method recommends the use of rat skin [97], it is also possible to identify corrosive substances and mixtures using RHE models composed of non-transformed epidermal keratinocytes. A range of RHE commercially available models such as the EpiSkin®, EpiDerm®, SkinEthic® and epiCS® are recommended for different categorization levels. These models are required to offer a viable multi-layered epithelium under a functional SC with validated barrier function, morphological properties and reproducibility. This method considers corrosive chemicals as those that are able to diffuse through or erode the SC and have cytotoxic effects on cells in the underlying layers [12]. These effects are evaluated by measuring cell viability immediately after chemical exposure using *in vitro* metabolic activity assays, as the 3-(4,5-dimethylthiazol-2yl)-2,5-diphenyl tetrazolium bromide (MTT) enzymatic conversion assay [12]. In addition to these methods, corrosion can also be assessed through the evaluation of the amount of damage inflicted by a chemical to artificial membranes that behave similarly to animal skin. Here, corrosion can be evaluated by color change of a chemical detection system after penetration through the barrier [98]. However, these methods can only

evaluate skin corrosion and are not able to distinguish skin irritants from chemicals that do not require classification [101]. Therefore, *in vitro* assessment of skin irritation is recommended by OECD guidelines and can be evaluated with RHE models, using a different protocol from corrosion evaluation, both in terms of exposure time and post-treatment incubation before MTT assay [10].

Cell metabolic activity studies using techniques such as MTT and alamar blue assays have been carried out in a high-throughput manner for the assessment of cytotoxicity of different compounds using an automated liquid handling system in 96-well plate cultures. However, these studies have used traditional 2D cell culture methodologies [102] instead of the recommended RHE cultures. It is, however, possible to apply low-throughput cell metabolic activity assessment techniques using RHE after a primary high-throughput assessment, as performed in a study of skin permeability enhancers in which only the most promising enhancers were screened for their irritation potential [7]. It is therefore necessary to develop reliable and scalable high-throughput methodologies compliant with OECD guidelines for *in vitro* assessment of skin irritation and corrosion.

Skin sensitization can be assessed *in vitro* with the KeratinoSens™ ARE-Nrf2 Luciferase test method. By using an immortalized human keratinocyte cell line that expresses luciferase after exposure to small electrophilic test substances such as skin sensitizers, this assay is able to evaluate a key biological event related to skin sensitization by the induction of a specific cell signalling pathway. The induction of the luciferase gene can then be quantified by luminescence detection [11]. This assay is suitable for high-throughput screening but its use alone is not sufficient for the assessment of skin sensitization, something that can only be thoroughly evaluated in combination with other testing methodologies. Some of the suggested techniques are comparisons with chemical analogues, the study of chemical reactivity with peptides or proteins, dendritic cell activation studies and *in silico* models [11,103–105].

Genotoxicity can be evaluated according to OECD guidelines using the *in vitro* micronucleus test. This method is used to investigate the effect of a chemical on cell division through the detection of chromosomal damage that was transferred to daughter cells [100]. This strategy has been applied for studying micronucleus formation with the EpiDerm™ RHE in a multi-laboratory study and suggested as a reliable assay for the study of cosmetic genotoxicity [99].

Cutaneous toxicity is a complex process and even though there have been significant improvements on *in vitro* methodologies for its evaluation, only a few protocols have been proven to be robust enough to gain recommendation in international guidelines. Moreover, these recommended methods acting alone are often not enough to gain a complete understanding of skin toxicity. Therefore, and according to the current shifting trend from *in*

vivo to *in vitro* methods in domains such as the testing of cosmetics, it is necessary to develop novel, integrative testing platforms for the assessment of skin toxicity that are reliable, versatile and can be implemented in multiple laboratories.

1.4. MICROFLUIDIC STRATEGIES FOR SKIN EMULATION

Due to the current needs for the development of more biologically relevant platforms for *in vitro* studies, the organ-on-a-chip concept has been proposed and described as a device that aims to model the physiological functions of tissues or organs through the use of cell culture in continuously perfused microfluidic systems [16]. These systems consist of microfluidic chambers where one or more cell types are usually cultured, and that can further be separated by porous membranes mimicking biological interfaces [106]. Moreover, it is possible to include biologically-relevant forces in the system such as peristalsis-like deformations and shear stress as well as to establish co-culture systems with microorganisms [107] in order to modulate cell and tissue behavior. Microfluidic devices for emulation of organs such as the lung [106], kidney [108,109], liver [110], bone marrow [111], gut [107,112] and skin [113,114] have been developed by different research groups in the past decade, with significant progress. These are versatile models that can be based on *in vitro* [106] or *ex vivo* [111] culture systems not only for recapitulation of biological features and processes [112] but also as pathophysiological models of disease [107,115].

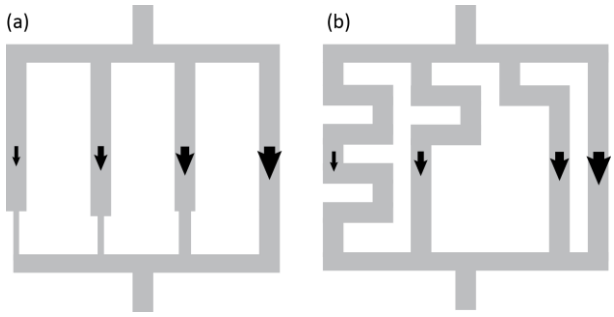

Figure 3: Microfluidic systems: (a) increasing channel width leads to an increasing flow rate; (b) decreasing channel length leads to an increasing flow rate;

Even though considerable research efforts have been focused on emulating different organs, only a reduced number of skin microfluidic systems have been developed so far, as summarized in Table 1. However, these are based on a wide variety of tissue models, from keratinocyte [116] or fibroblast [85,117,118] cultures to human skin equivalents [113,114] or *ex vivo* tissue [119–121] and have been applied for the study of processes such as transdermal

transport [113], wound healing [85] or to assess the response to shear stress [85,114,116–119], chemical agents [113,118–121] or electrical stimuli [85].

Early skin microfluidic devices were developed as simple models consisting of a flat glass surface in contact with polydimethylsiloxane (PDMS)-patterned microchannels fabricated by silicon photolithography and micromolding. Multiple-channel configurations were designed and the same pressure drop in channels of distinct widths was applied (Figure 3a) [117,118], allowing the over-time study of a range of linear [118] or logarithmically [117] increasing flow rates on fibroblast cell morphology [117] and detachment [118]. The first microfluidic model with human keratinocytes was designed to provide a range of shear conditions to cells cultured over a collagen-patterned surface. Channels were designed with different lengths, resulting in a linear flow rate increase (Figure 3b). This strategy allowed light microscopy analysis for cell morphology assessment, on-chip immunostainings and cell viability quantification using fluorescence microscopy [116].

A device allowing multiple laminar flows over a surface was produced and used to create a microfluidic wound healing model (Figure 2c). By using three inlets, a flow of trypsin/ethylenediaminetetraacetic acid (EDTA) could be established between two flows of PBS over a fibroblast monolayer, allowing the detachment of a well-defined cell portion. Afterwards, cell migration towards the centre of the wound was evaluated by microscopy under the influence of chemical migration promoters and inhibitors [95]

Recently, more sophisticated approaches have been developed to combine media perfusion and electrical stimuli on fibroblast cell cultures [85,122]. A microfluidic system for wound healing studies was fabricated in order to assess the effect of chemical and electrical stimuli on fibroblast migration. This chip was composed of a polymethyl methacrylate (PMMA) channel for medium flow and electrical stimulus attached to a tissue culture polystyrene (TCPS) dish for cell culture. A wound healing model was established with a modified barrier assay observed with time-lapse imaging. The electrical field inside the chip was measured in a non-invasive way using a Dermacorder (BioElectroMed Corp.) [122]. A different system was also developed to study the influence of fluid shear stress in combination with an electrical field stimulation on fibroblast cell cultures inside PDMS microchannels. This platform allowed the application of sequential or combinatorial stimuli with a peristaltic pump and a voltage source as well as real-time monitoring by optical microscopy and channel voltage measurements. Using this system, it was possible to establish an *in vitro* wound healing model and to find a cooperative effect of the two physical stimuli in study on fibroblast migration rate and direction [85].

Table 1: Types of assays that have been performed on-chip using skin microfluidic devices.

Stimulus	Skin model	On-chip assay	Ref.
Shear stress, chemical substance in culture medium (EGF)	WT NR6 mouse fibroblasts	Observation with inverted microscope	[118]
Shear stress	3T3 mouse fibroblast culture	Observation with inverted microscope	[117]
Shear stress	KC	Observation with inverted light and fluorescence microscope, live/dead assay and immunostaining	[116]
Chemical substance in culture medium (fetal bovine serum, phalloidin, cytochalasin D, rat epidermal growth factor)	3T3 mouse fibroblast culture	Wound formation and cell migration, observation with phase contrast inverted microscope	[95]
Electric field chemical substances (serum, β-lapachone)	3T3 mouse fibroblast culture	Observation with inverted microscope	[122]
Shear stress and electric field	DFC	Observation with phase contrast inverted microscope	[85]
Shear stress	SB, HSE	Skin sample collection	[114]
FAM-Tagged nucleotide solution on topical surface	HSE	Medium collection	[113]
Chemical substance in culture medium (doxorubicin)	HSE	Skin sample collection	[113]
Chemical substance in culture medium (troglitazone)	SB + liver microtissue aggregates	Skin sample and medium collection	[119]
Shear stress	SB + liver microtissue aggregates	Skin sample and medium collection	[119]
Chemical substance in culture medium (troglitazone)	SB + liver microtissue aggregates + endothelial cells	Skin sample and medium collection	[121]
Chemical substance in culture medium (troglitazone)	SB + liver microtissue aggregates + intestine + kidney	Skin sample and medium collection	[120]

DFC: Dermal fibroblast culture; EGF: Epidermal growth factor; KC: Keratinocyte culture; HSE: Human skin equivalent; SB: Skin biopsy.

In order to integrate 3D human skin equivalent models or skin biopsies in microfluidic systems, different skin-on-chip devices have been recently developed. A Multi-Organ-Chip (MOC) system allowing culture of different tissues in different compartments under static or dynamic conditions was fabricated with an on-chip pulsatile micropump to generate fluid flow (Figure

4a). This system was used to study a FT skin *in vitro* model (EpiDermFT®) cultured over a subcutaneous tissue biopsy as well as the behaviour of *ex vivo* skin and *ex vivo* single hair follicular units. The versatility of this device allowed not only submerged tissue culture but also the use of Transwell® systems integrated within the chip with skin at the air-liquid interface [114]. The same system was applied in a more integrative approach by combining tissues from multiple organs on the same chip as a co-culture system. Skin biopsies at the air-liquid interface were co-cultured in a two-organ-chip system with liver tissue [119,121] and in a four-organ-chip system with liver, intestine and kidney tissues for up to 28 days [120]. An innovative pumpless skin-on-chip device was also recently fabricated (Figure 4b), allowing the study of FT human skin equivalents at the air-liquid interface for up to three weeks. This system has been used not only for drug testing with histology and immunohistochemistry studies after skin sample removal but also for transdermal transport studies after medium collection. Moreover, in contrast to the MOC system, it was possible to control the medium flow rate with no need of a pump, by placing the chip on a rocking platform. Even though this strategy made it difficult to maintain the air-liquid interface at the skin sample surface, it may allow for an easier scale-up for testing a higher number of samples simultaneously, as it does not require pump and tubing systems for each sample [113].

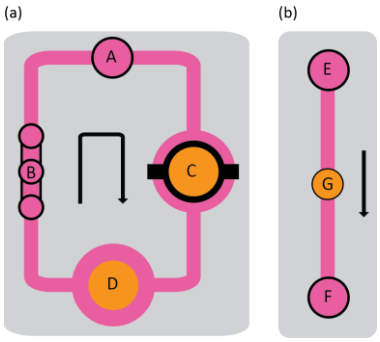

Figure 4: 3D skin microfluidic devices. (a) multi-organ-chip (adapted from [123]); (b) pumpless skin-on-chip (adapted from [113]); A: injection port; B: on-chip micropump; C: skin sample at the air-liquid interface on Transwell® system; D: skin sample submerged in circulating fluid; E-F: medium reservoirs; G: skin sample at the air-liquid interface on a membrane.

On-chip platforms for skin emulation have been proven to be versatile alternatives for the evaluation of different biological phenomena. Moreover, as they are more sophisticated than earlier *in vitro* models, they make it possible to study the combination of different stimuli and can be designed to be used with a wide range of skin models. However, most skin-on-chip devices using 3D culture methods similar to the ones recommended by international

guidelines only allow basic on-chip assays, providing skin or medium sample collection ability and requiring off-chip analysis. Even though some miniaturization and process automation has been accomplished, in order to develop high-throughput on-chip systems, less manipulation and more integration of testing methodology are required. Recently, novel strategies combining advanced high-throughput and organ-on-a-chip technologies [124,125] in combination with 3D bioprinting [124] have been reported, potentially contributing to the creation of novel skin-on-chip platforms. However, testing reliability and reproducibility still have to be proven in order to possibly include on-chip assays in international testing guidelines. Even though microfluidic devices may allow a more comprehensive emulation of biological events, it is necessary to find a balance between complexity and simplicity in order to make these systems easy to use and compatible with both research and regulatory needs.

However, even though plenty research efforts have been put in place for the development of organ-on-a-chip models, from our knowledge, only two systems integrating microfluidic 3D skin constructs have been developed so far. These were fairly simple systems, optimized for only one skin sample and posing several difficulties to scale up. However, as novel technologies combining high-throughput, organ-on-a-chip, and advanced fabrication technologies such as 3D bioprinting have been recently developed [124,125], it is now possible to create novel and more versatile devices for skin emulation.

CHAPTER 2: OBJECTIVES

In order to develop a skin-on-chip device useful for emulating phenomena such as transdermal transport, wound repair and skin toxicity in a high-throughput manner, the work performed in the scope of this thesis was focused on the production of a 3D *in vitro* skin model. This model, composed of fibroblasts entrapped in a photopolymerizable hydrogel system based on methacrylated hyaluronic acid (HAMA) and methacrylated pectin (PectMA), was aimed to be used as the dermal component of the device.

In order to successfully produce and integrate this skin model as part of the organ-on-a-chip system, several requirements need to be fulfilled, including: i) suitability for high-throughput applications, particularly in 96-well plate arrays; ii) possibility of being used as a photopolymerizable bioink for 3D printing to create structural complexity and allow automated fabrication of reproducible constructs; iii) ability to sustain fibroblasts in culture for several days, keeping them viable and metabolically active.

Therefore, and in order to design and produce a suitable skin model, the main objectives of this thesis were:

1. To purify and chemically modify biocompatible polymers, namely hyaluronic acid and pectin, to allow the development of a photopolymerizable hybrid hydrogel system;
2. To prepare and characterize hydrogel formulations with varying polymer compositions and ratios, envisioning the tunability of the mechanical properties of the developed system;
3. To functionalize the proposed materials with RGD peptides to provide the hydrogels with cell adhesive cues;
4. To evaluate the *in vitro* response of fibroblasts cultured within the hydrogel matrices, in terms of cell viability and ability to spread inside the hydrogels;

CHAPTER 3: MATERIALS AND METHODS

3.1. MATERIALS

Hyaluronic acid sodium salt (HA, Hyasis® 850P, Mw = 1.6 MDa) was obtained from Novozymes; Low-methoxyl (LM) citrus pectin (Classic CU701) was provided by Herbstreith & Fox. Methacrylic anhydride (MA, 276685) and 2-Hydroxy-4'-(2-hydroxyethoxy)-2-methylpropiophenone (Irgacure 2959) were purchased from Sigma.

3.2. PECTIN PURIFICATION

A 1% (w/v) LM pectin solution was prepared by dissolution in Hyclone™ endotoxin-free cell culture grade water (GE Healthcare). After dissolution, pH was adjusted to 6 and the solution was filtered using a succession of 0.8 µm, 0.45 µm and 0.22 µm mixed cellulose ester filter membranes (Millipore). Then, 2% (w/v) activated charcoal (Sigma) was added and the suspension was agitated (250 rpm) for 1h at room temperature and centrifuged at 60 000 g for 1h at 20°C (Beckman Avanti J-26 XP, Beckman Coulter). After discarding the supernatant, suspensions were ultracentrifuged at 120 000 g for 1h at 20°C (Beckman Optima, Beckman Coulter), decanted and filtered with 0.22 µm polyethersulfone filter membrane using a bottom top vacuum filter unit (Millipore). Finally, the resulting purified pectin solutions were frozen at -20°C, freeze-dried for 2 days (BenchTop Pro, VirTis) and stored at -20°C until further use.

3.3. SYNTHESIS OF METHACRYLATED HYALURONIC ACID

HA was methacrylated based on previously established protocols [126,127]. Briefly, HAMA was synthesised by reacting a 1% (w/v) HA solution prepared in tris-buffered saline solution (TBS, 100 mM Tris, Amresco, 150 mM NaCl, VWR, pH 8) with a 43-fold molar excess of MA. The mixture was allowed to react for a total of 6h under magnetic stirring with stepwise additions of MA (37.5% of total MA volume at 0h, 37.5% at 1.5h and 25% at 3h). This reaction was performed in an ice bath and pH was maintained at 8-8.5 by dropwise addition of a 5M sodium hydroxide (NaOH) solution (VWR). HAMA was then precipitated and washed in ethanol at 4°C, left to dry for 1h and re-dissolved overnight in deionized water. The obtained HAMA solution was purified by dialysis (MWCO 3.5 kDa, Spectra/Por®, Spectrumlabs) against decreasing concentrations (7.5, 6.25, 5, 3.75, 2.5, 1.25, 0 g/L) of sodium chloride (NaCl) in deionized water for two days, with water renewal 3 times a day. The HAMA solution was then frozen at -20°C, freeze-dried for 2 days at -80°C (BenchTop Pro, VirTis) and stored at -20 °C until further use.

3.4. Synthesis of Methacrylated Pectin

PectMA was prepared and kindly provided by Rúben Pereira and Filipa Sousa from i3S/INEB (detailed protocol to be published elsewhere).

3.5. Preparation of HAMA/PectMA hydrogels

3.5.1. Preparation of HAMA/PectMA hydrogel precursor (pre-polymer) solutions and functionalization with RGD

Irgacure 2959 (photoinitiator) solutions were prepared at a final concentration of 0.05% (w/v) in either 0.9% NaCl (pH 5.5) in deionized water or PBS (pH 8.5) and used to separately dissolve HAMA and PectMA. Then, HAMA and PectMA solutions were mixed together at a 1:1 ratio yielding final pre-polymer solutions with defined concentrations of each polymer.

In order to prepare Arg-Gly-Asp (RGD)-functionalized pre-polymer solutions, thiolated RGD peptides (CGGGGRGDSP, MW=861.88 $gmol^{-1}$, Genscript) were dissolved in the pre-polymer solutions at final concentrations of 1 mM and 2 mM and allowed to react for 20h at 20°C under 1400 rpm agitation (Thermomixer comfort, Eppendorf).

Herein, different pre-polymer concentrations were tested, as described in Table 2.

TABLE 2: COMPOSITION OF PRE-POLYMER SOLUTIONS USED IN THIS WORK. DIFFERENT FORMULATIONS WERE PREPARED WITH VARYING HAMA, PECTMA AND RGD CONCENTRATIONS.

HAMA % (w/v)	PectMA % (w/v)	RGD (mM)	Dissolved in 0.05% Irgacure in
0.125	0.125	0	0.9% NaCl
0.25			
0.75			
1.5			
0.75	0	0	0.9% NaCl
	0.125		
	0.25		
0.75	0.125	0	PBS pH 8.5
		1	
		2	

3.5.2. Fabrication of HAMA/PectMA hydrogels

Hydrogel disks composed of a mixture of HAMA and PectMA were prepared by photocrosslinking with ultraviolet (UV) radiation. For each disk, 35 µl of pre-polymer solution was transferred to a polytetrafluoroethylene (PTFE) surface (Figure 5 a) and compressed with a

glass slide using a 750 µm spacer (Figure 5 b). UV light (Blue Wave 200, Dymax) intensity under the slide was calibrated (Accu-cal®-30, Dymax) to 7 mW/cm^2 and then applied to pre-polymer solutions for 60 seconds (Figure 5 (b)). The glass slide was then carefully removed from the surface and disks were detached using a spatula.

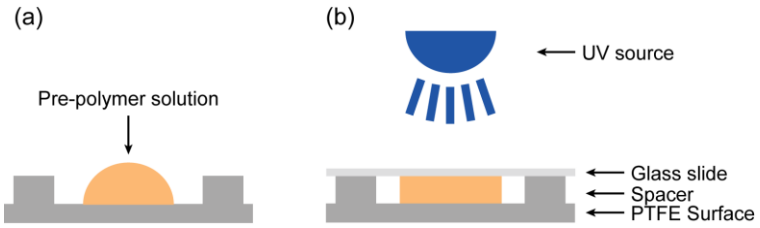

Figure 5: P*reparation of HAMA/PectMA hydrogels (a) pre-polymer solutions were pipetted over a PTFE surface, (b) pre-polymer were photocrosslinked using UV light.*

3.6. Physicochemical characterization of developed hydrogels

3.6.1. ^{1}H NMR characterization of hydrogel precursor (pre-polymer) solutions

Methacrylation efficiency was evaluated by ^{1}H Nuclear magnetic resonance (NMR). HAMA was dissolved in deuterium oxide (^2H_2O) (Sigma) overnight with agitation (4°C, 1400 rpm) at a concentration of 0.5% (w/v). ^{1}H NMR spectra were then recorded at 70°C using an NMR spectrometer (Bruker Avance III, Bruker).

Methacrylation efficiency of PectMA was evaluated according to a detailed protocol (to be published elsewhere).

3.6.2. Rheological evaluation (shear moduli)

The rheological behaviour of hydrogels was evaluated using a Kinexus Pro rheometer (Malvern Instruments, Malvern, UK). Hydrogel disks were prepared from 35 µl of precursor solution with a 750 µm initial height (distance from the PTFE surface to the glass slide) defined by a spacer and incubated at 37°C in 500 µl Dulbecco's Modified Eagle Medium-HEPES (DMEM-HEPES, Sigma) supplemented with 10% Fetal Bovine Serum (FBS) in wells of 24-well plates. After 1 and 3 days of incubation, disks were removed from the wells, punched into cylinders with 4 mm diameter, placed between parallel plate geometries of the rheometer and compressed to 80% of their height. Shear elastic modulus was evaluated by frequency sweep tests at 37°C in a water-vapour saturated environment with constant 1% strain from 0.01-10 Hz.

3.7. Preparation of cell-laden HAMA/PectMA hydrogels

3.7.1. Cell culture

Human Dermal Neonatal Fibroblasts isolated from foreskins of healthy male newborns (HDNFs, Zenbio) were cultured in Dulbecco's Modified Eagle Medium high glucose,

GlutaMAX™, 110 mg/L sodium pyruvate (31966, Gibco) supplemented with 10% (v/v) Fetal Bovine Serum (FBS, 10270, Gibco), 1% (v/v) Penicillin/Streptomycin (Biowest), 1% (v/v) Amphotericin B (Capricorn Scientific). Cells were maintained at 37°C, 5% CO_2 atmosphere in a humidified incubator and trypsinized (0.05% trypsin/EDTA solution) at 90% confluence. For all experiments, fibroblasts were used at passages 5-9.

3.7.2. Cell entrapment within HAMA/PectMA hydrogels

Hydrogel pre-polymer solutions were prepared as described above, pre-warmed at 37°C and HDNFs were suspended in those solutions at a final cell density of 10^7 cells/mL.

Cell-laden pre-polymer solutions were then photopolymerized into 20 µL hydrogel disks using a 500 µm spacer. Disks were then transferred to 24-well plates, immersed in 500 µL of complete DMEM and cultured in a humidified incubator at 37°C, 5% CO_2. Medium was refreshed after 1 hour and every 3 days in culture. Cell viability and synthesis of extracellular matrix (ECM) components were then evaluated up to 7 days in culture.

3.8. Biological characterization of cell-laden hydrogels

3.8.1. Evaluation of cell-laden hydrogel disk area

Hydrogel area was evaluated by image analysis. In brief, culture medium was removed from wells containing hydrogel disks after 1, 3, and 7 days in culture and images of the disks were recorded with 0.63x magnification using a stereo microscope (SZX16, Olympus). Disk area was then measured using FIJI software (ImageJ 1.51d).

3.8.2. Cell-laden hydrogel dissolution and cell retrieval

Hydrogel matrices were washed with PBS, transferred to individual Eppendorf tubes and dissolved by incubation with a 1000 U/mL hyaluronidase (Sigma), 50 U/mL pectinase (Sigma), 2.5% (w/v) trypsin 5 mM EDTA solution in PBS for 5 minutes or until dissolved at 37°C under 1400 rpm agitation (Thermomixer comfort, Eppendorf). After hydrogel dissolution, cell suspensions were centrifuged at 10 000 rpm for 5 minutes. Supernatants were discarded and cell pellets were washed with 500 µL PBS and centrifuged twice (10 000 rpm, 5 minutes). After the final centrifugation, cells were re-suspended in PBS, counted using a Neubauer chamber and cell numbers per hydrogel were determined.

3.8.3. Evaluation of cell metabolic activity (resazurin reduction assay)

Cell metabolic activity was evaluated using the Resazurin-reduction assay after 1, 3 and 7 days in culture. Hydrogels were transferred to wells of 24-well plates containing 500 µL of complete DMEM with 20% (v/v) resazurin (Sigma) and incubated for 2h at 37°C, 5% CO_2 in a humidified incubator. Then, medium was transferred to wells of a black 96-well plate (100 µL/well) and fluorescence was recorded (530 nm λ_{ex}, 590 λ_{em}) using a microplate reader (Synergy Mx, BioTek). Fluorescence levels were then normalized for the number of cells retrieved from each hydrogel after dissolution.

3.8.4. Evaluation of cell viability by Live/Dead assay

After incubation for 1, 3, and 7 days, hydrogel disks were transferred to wells of a 24-well plate containing 500 µL of 2 µg/mL Calcein (Invitrogen), 2.5 µg/mL Propidium Iodide (Sigma) solution in TBS for 30 minutes. Then, disks were washed twice in TBS and observed under a confocal microscope (Leica TCS-SP5 AOBS, Leica Microsystems), using laser wavelengths of 488 nm (green) and 561 nm (red). Live cells were stained green and dead cells stained red.

3.8.5. Characterization of cell phenotype and ECM production by immunocytochemistry

For evaluating cell cytoskeleton, F-actin distribution was stained using the conjugated probe phalloidin/Alexa Fluor® 488 (Molecular Probes-Invitrogen, 1:40). For assessing ECM synthesis and deposition, rabbit anti-fibronectin (f3648, Sigma, 1:400) primary antibody was used. Goat anti-rabbit Alexa Fluor® 594 F(ab')$_2$ fragment (Molecular Probes-Invitrogen, 1:1000) was used as secondary antibody. All antibodies were diluted in 1% (w/v) bovine serum albumin (BSA) in 7.5 mM $CaCl_2$ in TBS. After being cultured in HAMA/PectMA hydrogels for 1, 3 and 7 days, cell-laden hydrogels were washed twice with 7.5 mM $CaCl_2$ in TBS, fixed with 4% (v/v) paraformaldehyde (Electron Microscopy Sciences) in TBS for 20 minutes, washed twice again and kept at 4°C. Cells were then permeabilized by incubation with 0.1% (v/v) Triton X-100 in 7.5 mM $CaCl_2$ in TBS, washed 3 times with 7.5 mM $CaCl_2$ in TBS, blocked with 1% (w/v) BSA in 7.5 mM $CaCl_2$ in TBS for 1h and incubated with primary antibody at room temperature for 4h. Samples were then washed 3 times with 7.5 mM $CaCl_2$ in TBS and incubated with secondary antibody and Phalloidin/Alexa Fluor® 488 in 1% BSA for 45 minutes. After washing 3 times with 7.5 mM $CaCl_2$ in TBS, cell nuclei were counterstained with Vectashield mounting medium with 4',6-diamino-2-phenylindole dihydrochloride (DAPI) (H-1200, Vector) before visualization using a confocal microscope (Leica TCS-SP5 AOBS, Leica Microsystems).

3.9. STATISTICAL ANALYSIS

Quantifications are expressed as mean ± standard error mean (SEM). A difference between experimental groups was considered significant with a 95% confidence interval whenever $p<0.05$. For comparisons between hydrogel formulations and timepoints, the two-way ANOVA statistical test was applied.

CHAPTER 4: RESULTS AND DISCUSSION

4.1. PREPARATION OF HAMA/PECTMA HYDROGEL PRECURSOR (PRE-POLYMER) SOLUTIONS

Hyaluronic acid (HA) is a biocompatible, biodegradable and viscoelastic non-sulfated glycosaminoglycan composed of D-glucuronic acid and N-acetyl-D-glucosamine (Figure 6a) [128,129]. It is an ECM component biodegradable by hyaluronidase and its high abundance in skin makes this organ its largest reservoir in the body [130,131]. HA exists in both dermis and epidermis [132] and provides binding sites for CD44, a molecule expressed by cells such as fibroblasts [133]. Even though it is abundant in natural tissues, one major advantage of HA is that it can be produced using bacteria (e.g. *Streptococci* or *Bacillus subtilis*) by fermentation or direct isolation, allowing the generation of large material quantities in a reproducible way [132,134].

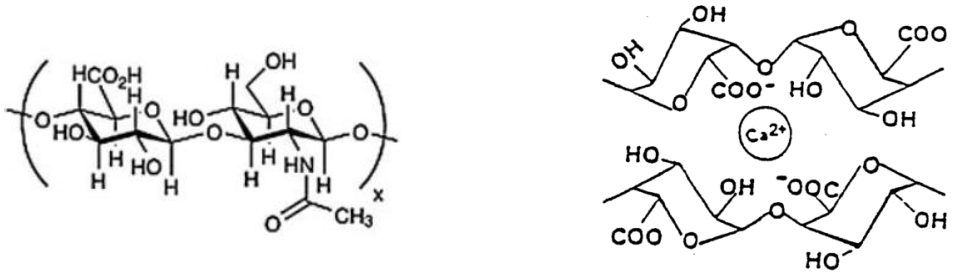

Figure 6: (a) hyaluronic acid chemical structure [135] (b) pectin chemical structure and coordination with Ca^{2+} ions [136]

Pectin (Figure 6b), on the other hand, is a polysaccharide composed of alternating α-L-(1-4)-guluronate residues and α-D-galacturonate residues [137]. Low-methoxyl pectins form gels in the presence of Ca^{2+} [136], as they are able to coordinate divalent cations forming "egg-box" molecular structures [137] which allows this material to form hydrogels via internal [138] or external [139] gelation mechanisms.

Herein, both polymers were methacrylated in order to make them photocrosslinkable and mixed to form pre-polymer solutions that would benefit from both UV crosslinking by free radical polymerization and external gelation of PectMA by calcium coordination.

4.1.1. METHACRYLATION OF HA

In order to create a covalently photocrosslinkable two-polymer hydrogel system, HA was modified through a reaction with methacrylic anhydride. This reaction of unmodified HA with methacrylic anhydride under alkaline conditions is one of the simplest processes used for the

modification of HA [140]. Methacrylate-modified materials have been receiving great attention in the field of tissue engineering, owing to their overall good cytocompatibility [141,142] as well as adjustable mechanical properties [143]. This modification generates photocrosslinkable materials through the addition of methacrylate moieties to the polymer backbone, which react upon exposure to a light source (UV light in the present work), establishing bonds that connect adjacent molecules within a polymeric matrix. Several factors can affect the efficiency of the methacrylation reaction, including the reaction time, as well as the excess amount of MA and the molecular weight of the unmodified (initial) polymer [126,142].

Herein, HA modification was confirmed by ^{1}H-NMR spectroscopy. The spectrum obtained for HAMA (FIGURE 7) displayed the characteristic peaks of the two protons of the double bond region of MA (δ 5.75-6.19 ppm), which are absent in the unmodified HA. The degree of methacrylation of HAMA was calculated as the ratio between the relative peak integrations of methacryloyl group protons (δ 5.75-6.19 ppm) and HA methyl protons (δ 2 ppm) and determined to be 8% (Figure 7).

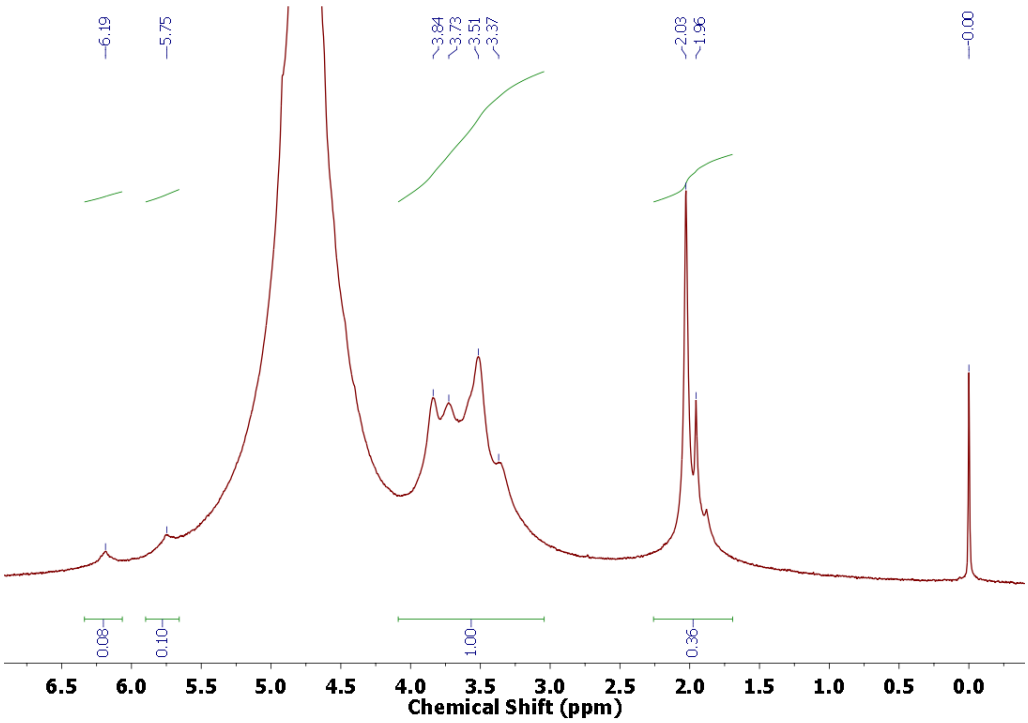

Figure 7: NMR spectrum of HAMA.

4.2. *Hydrogel formation and characterization*

4.2.1. *Influence of PectMA and HAMA* concentrations and ratios

In order to preliminarily screen the influence of PectMA content on hydrogel properties and to define hydrogel mixture concentrations to be further studied, hydrogel formulations of varying PectMA concentrations ranging from 0% to 1.5% were evaluated after overnight incubation at 37°C in DMEM-HEPES. For this purpose, hydrogels were produced with a constant concentration of HAMA (0.75%, w/v) and the shear elastic moduli (G') of different formulations were assessed. The obtained samples exhibited a range of G' from less than 100 Pa to more than 1.5 kPa, increasing with higher PectMA content (Table 3).

Table 3*: Preliminary assessment for the optimization of % PectMA in hydrogel disks.*

HAMA % (w/v)	PectMA % (w/v)	G' (Pa)
0.75	0	68
	0.5	709
	1.5	1521

Hydrogel moduli are able to Fibroblast ability to spread and proliferate is influenced by matrix stiffness, as networks with high moduli (>1 kPa) can act as a physical barrier to cells which is not evident in softer formulations [144]. Indeed, for hydrogels with shear moduli ranging from 50 to 1200 Pa, fibroblast morphology has been reported to be radically altered, with cell spreading being promoted in hydrogels with lower modulus and inflammatory pathways being triggered for cells cultured in stiffer matrices [145]. Compliant matrices with moduli ≤120 Pa have also been shown to promote cell proliferation and lead to mesenchymal stem cell aggregation [146]. As formulations with increasing concentrations of PectMA (0.5 and 1.5%, w/v) rendered matrices stiffer, and in order to produce hydrogels with low G', the influence of % PectMA between 0% and 0.25% was further evaluated using lower PectMA concentrations, in the range of 0% to 0.25% after 1 and 3 days of incubation at 37°C in DMEM-HEPES supplemented with 10% FBS. Here, a significant increase in G' values was observed with increased % PectMA in all three formulations analysed (0, 0.125 and 0.25% PectMA with constant 0.75% HAMA, Figure 8), which shows a strong dependency of this property on the PectMA content of the hydrogels. Moreover, for hydrogels with the highest PectMA content (0.25%), a significant increase in G' was noticeable between day 1 and day 3.

The observed stiffening of hydrogels with higher PectMA concentrations might be due to the fact that besides being able to polymerize by covalently linking methacrylate moieties, this polymer is also able to coordinate Ca^{2+} [147,138] ions that are also present in culture medium. The medium used contains 1.8 mM calcium chloride, according to the manufacturer. The ionic crosslinking promoted by Ca^{2+} leads to a secondary gelation process that might occur in a longer timeframe than the initial photocrosslinking. These results suggest that for higher PectMA concentrations the hydrogel system might take longer than 1 day to stabilize in culture medium, whereas for lower PectMA concentration this phenomenon is no longer noticeable.

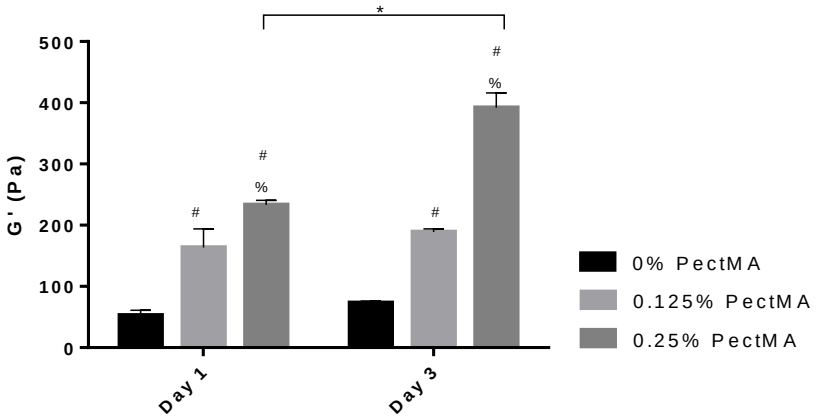

Figure 8: E*ffect of % PectMA on shear elastic modulus after 1 and 3 days of incubation in DMEM-HEPES with* 10% FBS. Legend: symbols denote statistically significant differences ($p<0.05$) from 0% PectMA (#), 0.125% PectMA (%), day 1 (*), n=4

Furthermore, in order to investigate the influence of HAMA on the mechanical behaviour of developed hydrogels, disks were fabricated with HAMA content ranging from 0.125% to 1.5%, while keeping PectMA constant at 0.125%.

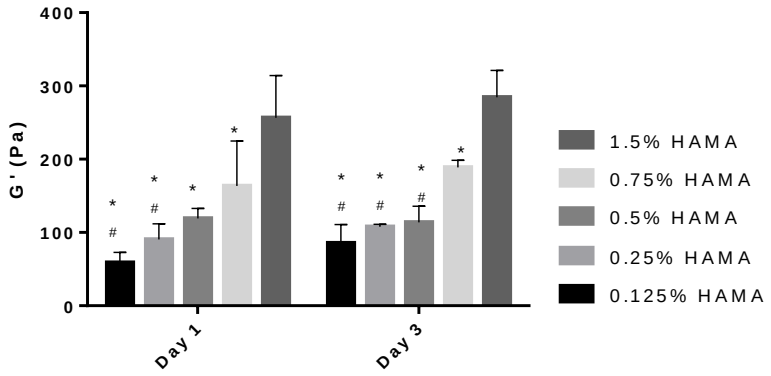

Figure 9: E*ffect of % HAMA on shear elastic modulus after 1 and 3 days of incubation in DMEM-HEPES* 10% FBS. Legend: symbols denote statistically significant differences ($p<0.05$) from 1.5% HAMA (*), 0.75% HAMA (#), n=4

Similar to what happened when %PectMA was increased, higher HAMA content in pre-polymer solutions led to hydrogels with higher G' (Figure 9). By day 1, G' values varied between 68 and 264 for the lowest (0.125% HAMA) and the highest (1.5% HAMA) concentrations of HAMA, respectively. However, modifying %HAMA resulted in no noticeable G' variations from day 1 to day 3, in opposition to observations made when increasing PectMA content from 0.125% to 0.25%. Indeed, a slight increase in PectMA led to a more than double G' after 3 days of incubation (Figure 8) while an increase of 0.75% HAMA resulted in stable hydrogels with no G' variations between the two timepoints (Figure 9).

HAMA content is known to have an influence in hydrogel mechanical properties as both compressive and shear moduli have been shown to increase with increasing concentrations [143,148]. This higher shear modulus has been suggested to be due to a higher density of crosslinks within the polymeric network [148]. Indeed, using this system, a range of hydrogel formulations could be prepared with tuneable moduli by varying polymer concentrations and ratios. In addition, as HA and pectin solutions often present distinct viscosity levels, with hyaluronic acid [149] being more viscous than pectin [150], viscosity could possibly become tuneable by adjusting the aforementioned parameters.

4.2.3. Influence of the solution used to prepare pre-polymer solutions

In order to modify methacrylated polymers with thiolated RGD at a basic pH [151,152], pre-polymer solutions were prepared at pH 8.5 in PBS and properties of the resulting hydrogels were compared with the ones of disks fabricated at pH 5.5 0.9% NaCl solutions. Herein, the influence of the two solutions used for dissolving both PectMA and HAMA on the shear elastic moduli of the developed hydrogels was evaluated. After 1 and 3 days of incubation at 37°C in DMEM-HEPES supplemented with 10% FBS, slightly higher moduli were observed in hydrogels prepared with PBS (Figure 10). However, no significant differences were noticeable between the two formulations at each time point or between the two timepoints for each formulation, supporting earlier observations and showing that hydrogels containing 0.75% HAMA and 0.125% PectMA are stable in culture medium over time.

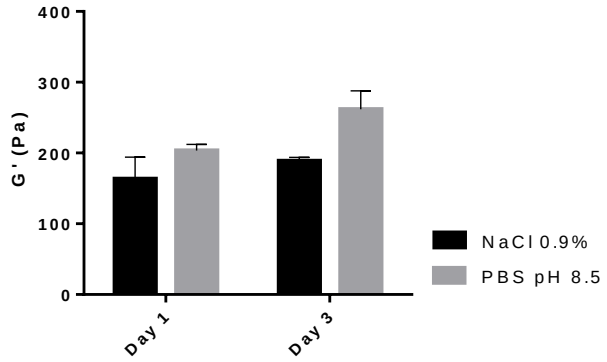

Figure 10: Influence of solvent on shear elastic modulus of hydrogel disks incubated in DMEM-HEPES 10% FBS at 37°C for 1 and 3 days, n=4

4.2.4. Influence of RGD modification

After obtaining a hydrogel system with adequate mechanical properties and stability in culture medium, pre-polymer solutions were modified with RGD peptides in order to promote cell adhesion [138,153]. Modifications of HA [154–156] and pectin [138,150] with RGD peptides have been described in the past using different protocols. However, as both polymers used herein had been previously modified with methacrylate moieties, a Michael-type addition reaction was conducted between thiolated RGD peptides and methacrylates. This type of reaction takes place between nucleophilic Michael donors (e.g. thiols of thiolated RGD peptides) and Michael acceptors (e.g. methacrylate groups of HAMA and PectMA) [157]. Considering that methacrylate groups are known to show slower reaction rates than other moieties such as acrylates [157], reaction was conducted for 20 hours at an alkaline pH (8.5). The high pH level is important to enhance reaction kinetics by increasing thiol deprotonation in solution [152,158,159], promoting the reaction with the Michael acceptor. Moreover, as pre-

polymer solutions were photopolymerized with UV light, thiol deprotonation by free radicals and further reaction with the polymer chains was also expected to occur [160].

Indeed, hydrogels containing RGD peptides were successfully fabricated with final RGD concentrations of 1 and 2 mM and shear elastic moduli were evaluated after 1 and 3 days of incubation in culture medium (Figure 11).

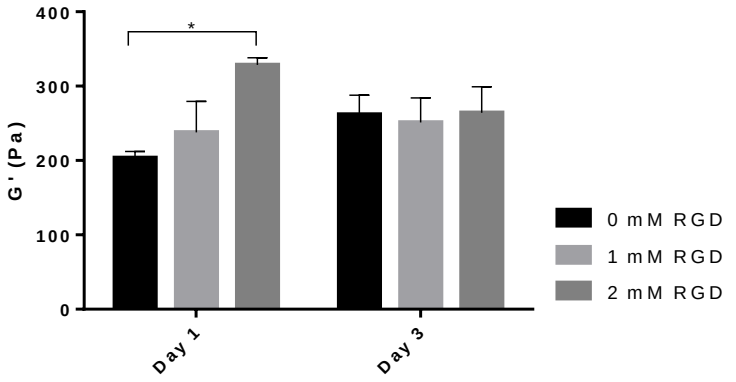

Figure 11: Influence of RGD modification on shear elastic modulus of hydrogel disks incubated in DMEM-HEPES with 10% FBS at 37°c for 1 and 3 days. Legend: symbols (*) denote statistically significant differences ($p<0.05$), n=4

After incubation in DMEM-HEPES 10% FBS for 1 day, hydrogels containing 2 mM RGD exhibited higher stiffness levels when compared with gels with no modification (Figure 11). However, this difference was no longer noticeable after 3 days. These results suggest that the amount of methacrylate groups that reacted with RGD peptides was not enough to inhibit hydrogel photopolymerization or decrease its stiffness by reactive site occupation. Indeed, RGD functionalization of hydrogels by Michael addition reaction has been reported to result in hydrogels with similar mechanical properties [161,162], whereas pectin hydrogels functionalized with RGD by carbodiimide chemistry have shown increased shear moduli [138].

Overall, the modification of the polymers used herein through the addition of RGD peptides did not result in significant alterations of the matrix stiffness, supporting the use of the material concentrations proposed above (0-0.125 %PectMA and 0.125-1.5 % HAMA) for the entrapment of fibroblasts and further evaluation of the biological performance of the system.

4.3. *IN VITRO CELL BEHAVIOUR*

4.3.1. *CELL NUMBERS WITHIN HYDROGEL MATRICES*

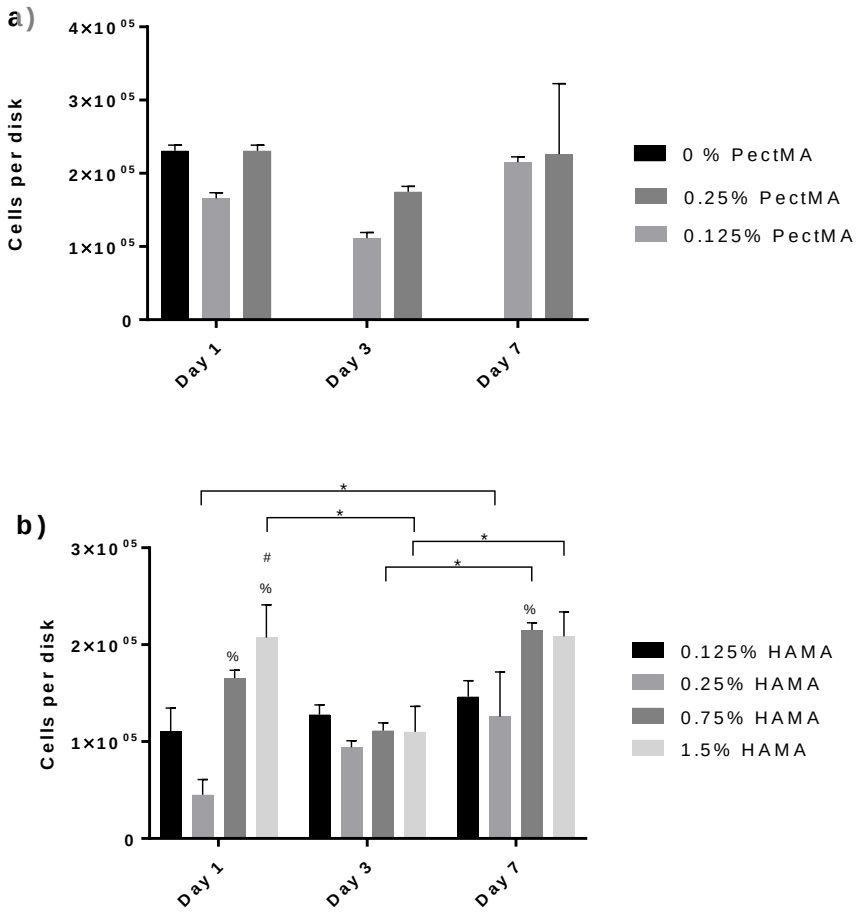

Figure 12: Cell numbers within each hydrogel disk after 1, 3 and 7 days in culture as a function of (a) %PectMA, with constant 0.75% HAMA (w/v); (b) %HAMA, with constant 0.125% PectMA (w/v) Legend: Symbols denote statistically significant differences ($p<0.05$) from different timepoint (*), 0.125% HAMA (#), 0.25% HAMA (%), n=3

The presence of encapsulated cells had a noticeable influence on hydrogel behaviour, as it was only possible to evaluate the number of cells encapsulated in hydrogels composed only of 0.75% HAMA (0% PectMA) on day 1. Soon after, these hydrogels without pectin started losing their integrity, making it impossible to adequately transfer them to Eppendorf tubes and quantify the cell number after 3 and 7 days in culture. Interestingly, all formulations composed of a mixture of HAMA and PectMA kept their integrity for the whole duration of the experiment, showing that the presence of PectMA is necessary, even at low concentrations (i.e. 0.125%), to keep the integrity of 0.75% HAMA hydrogel disks in culture for 7 days. Yet, for

formulations that kept their integrity with 0.75% HAMA, a further increase in PectMA content from 0.125% to 0.25% did not have a noticeable effect on the number of cells retrieved from the matrices and cell numbers were kept approximately constant throughout the 7 days (Figure 12 (a)). It is worth to mention, however, that a notable increase of shear elastic modulus was verified on hydrogels containing 0.125% PectMA when compared with formulations composed only of 0.75% HAMA, which might have been crucial to allow gel stability in culture. Indeed, hydrogels composed only of HAMA are expected to establish covalent bonds only between methacrylate moieties of HAMA chains whereas by adding PectMA, links not only between methacrylates of the same polymer but also between HAMA and PectMA are likely to occur. Moreover, as PectMA is able to undergo crosslinking by Ca^{2+} ions present in culture medium, a secondary stiffening is expected to contribute to higher overall hydrogel integrity. Therefore, the existence of two crosslinking steps may constitute an explanation for the reinforcement of the developed HAMA/PectMA hydrogels, which exhibit a better stability in aqueous environment over time, as observed herein.

On the other hand, increasing the amount of HAMA seems to lead to an increase in the number of cells entrapped within the hydrogel matrix on day 1, with significantly higher cell numbers on hydrogels with higher HAMA content (Figure 12 b). When comparing the behaviour of formulations with increasing HAMA content over time during the 7 days of culture, no common trend was noticeable regarding the number of cells retrieved. Indeed, the cell content of formulations containing 0.125% HAMA was approximately constant, while hydrogels containing 0.25% HAMA and 0.75% showed an increase in the number of encapsulated cells. Moreover, the formulations containing 1.5% HAMA exhibited a decrease in cell number after 3 days in culture which was followed by an increase on day 7. Overall, the highest cell number was registered in the formulation with the highest concentration of HAMA (1.5%), after 1 day.

Interestingly, for some formulations (0.75% HAMA, 0% PectMA; 0.75% HAMA, 0.25% PectMA; 1.5% HAMA, 0.125% PectMA), the number of cells counted after hydrogel dissolution was slightly higher than the initial number of cells loaded onto the hydrogel disks. This might be related to either cell embedding, disk dissolution or cell counting protocols. Even though several measures were implemented in order to minimize sources of error, factors such as the presence of small bubbles in the cell suspension mixed with pre-polymer solutions might have contributed to these unexpected results by respectively increasing the cell concentration in the hydrogels or leading to an overestimation of cell numbers. A possible alternative to this protocol would be to quantify total DNA content within using the Quant-it™ PicoGreen®

dsDNA assay kit (Invitrogen). Unexpectedly, cell number retrieved from hydrogels containing 0.25% HAMA / 0.125% PectMA on day 1 were lower when compared to other formulations with either higher or lower HAMA content.

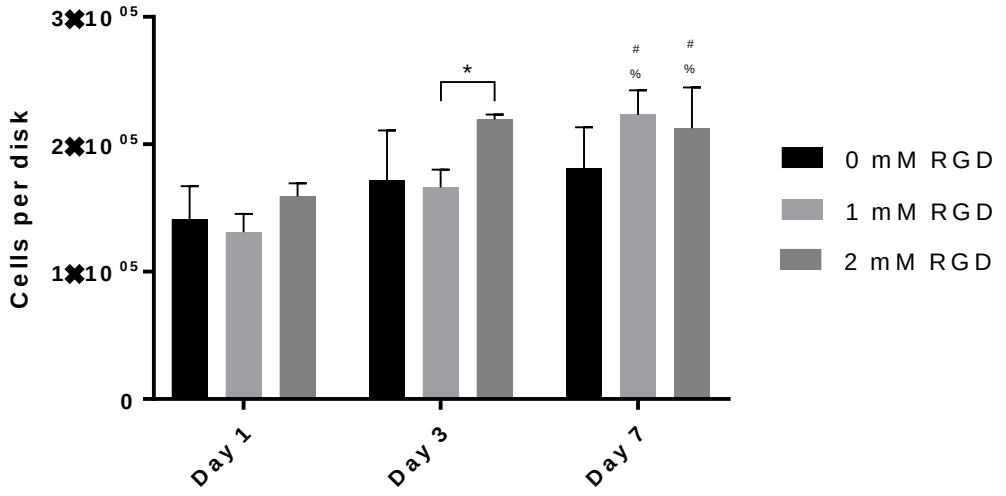

Figure 13: Cell numbers within each hydrogel disk after 1, 3 and 7 days in culture as a function of RGD concentration. Legend: Symbols denote statistically significant differences ($p<0.05$) from 1 mM RGD (*), day 1 (#), day 3 (%), n=3

Furthermore, cellular content was also assessed in RGD-modified hydrogels. After 1 day of culture, no differences were observed between non-functionalized hydrogel matrices and RGD-modified hydrogels. Nonetheless, functionalization of hydrogel formulations with RGD peptides led to an increase in cell numbers observed on day 7, which was not verified for cells cultured in non-functionalized hydrogel matrices (Figure 13). This suggests that cells cultured on RGD-functionalized hydrogels might preserve their proliferative capacity over time in culture.

4.3.2. DISK AREA VARIATION OVER TIME

In order to evaluate the effect of cells cultured on different hydrogel matrices on disk macroscopic integrity, hydrogel area was observed and measured after 1, 3 and 7 days in culture for varying % PectMA (Figure 14) and % HAMA (Figure 15). Hydrogel disks made out of non-functionalized polymers showed no considerable area variations with increasing time in culture. However, an increase in polymer content, particularly HAMA, led to higher disk areas, noticeable since day 1.

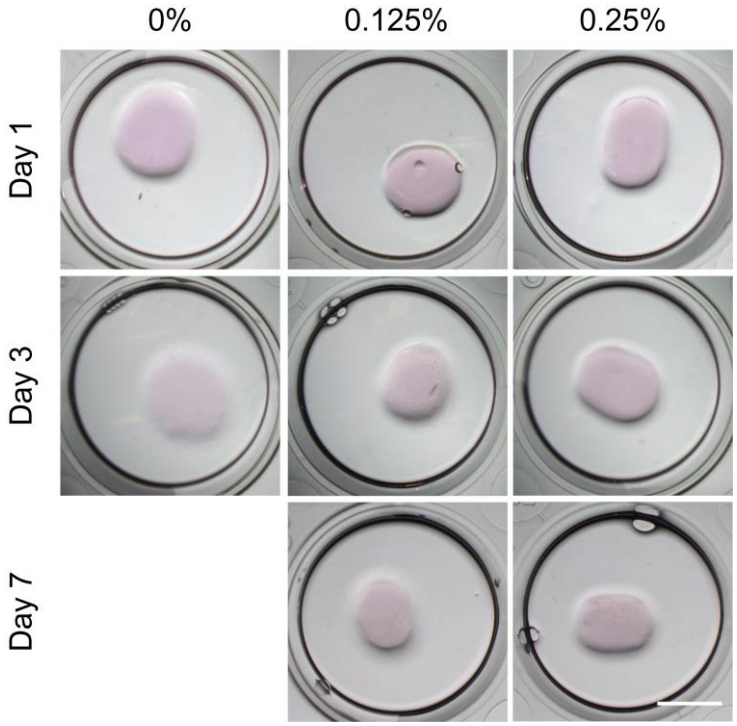

Figure 14: Macroscopic view of cell-laden HAMA/PectMA hydrogels with varying %PectMA after 1, 3 and 7 days in culture. Scale bar = 5 mm.

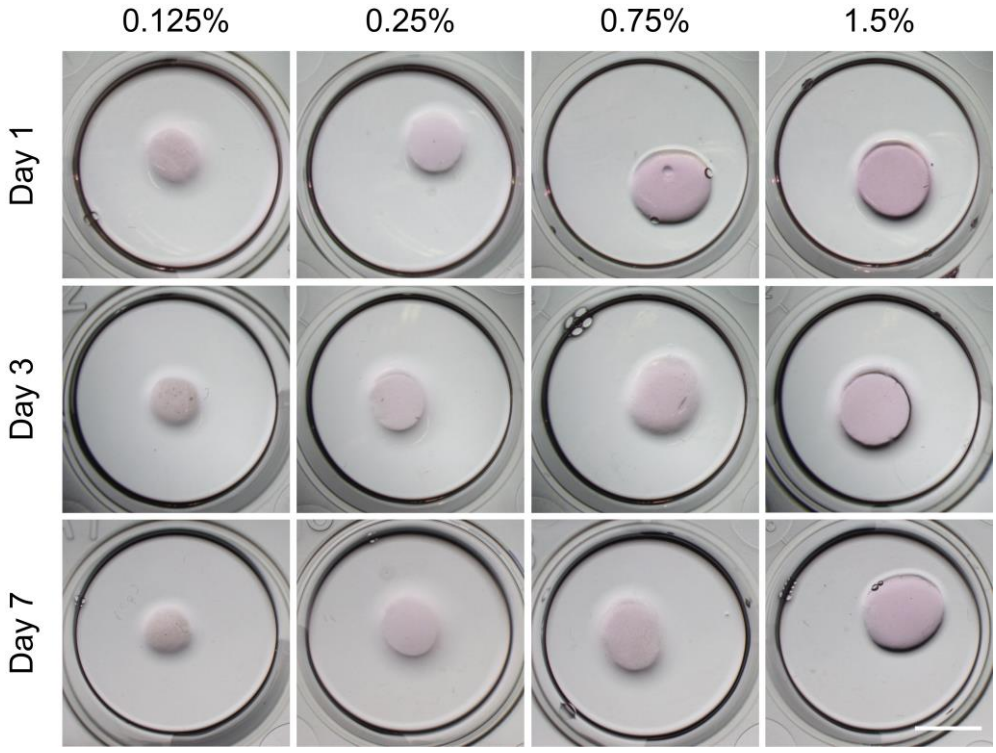

Figure 15: Macroscopic view of cell-laden HAMA/PectMA hydrogels with varying %HAMA after 1, 3 and 7 days in culture. Scale bar = 5 mm

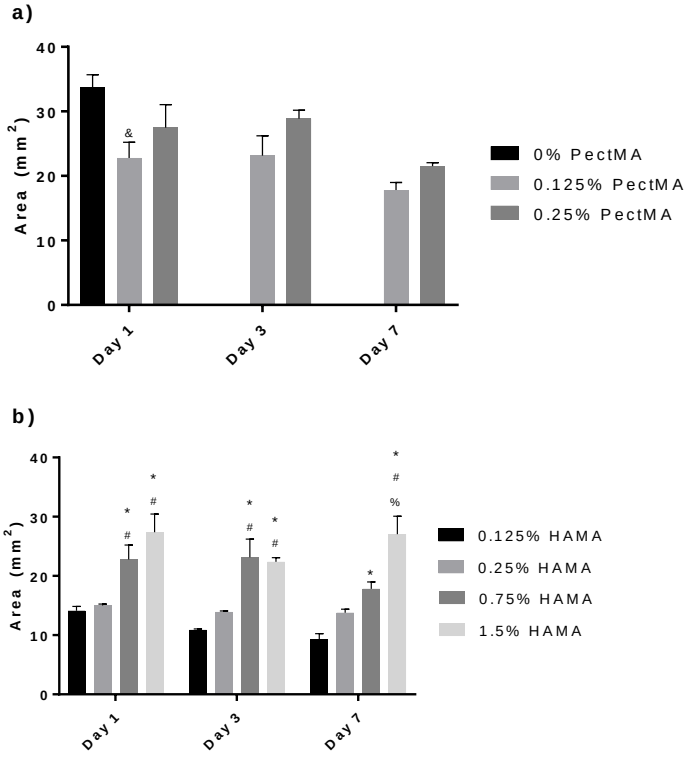

Figure 16: Influence of polymer concentration on cell-laden hydrogel disk area (a) variation of PectMA content with 0.75% HAMA; (b) variation of HAMA content with 0.125% PectMA. Legend: symbols denote statistically significant differences ($p<0.05$) from 0% PectMA (&), 0.125% HAMA (*), 0.25% HAMA (#), 0.75% HAMA (%), n=3

However, contrarily to the behaviour of hydrogels made solely out of methacrylated polymer mixtures, the functionalization of 0.75% HAMA/0.125% PectMA formulations with RGD peptides led to a contraction of the hydrogel matrix after being cultured with cells, as noticeable by a decrease in disk area after 3 and 7 days (Figure 18). Even though hydrogel contraction was present in all three formulations (0 mM, 1 mM and 2 mM), a significantly lower disk area was noticeable after 3 days in culture in 2 mM RGD disks, whereas it was only observable after 7 days in 0 mM and 1 mM formulations. Nevertheless, hydrogel disks functionalized with 1 and 2 mM RGD and cultured with HDNFs for 7 days displayed an area of 37% and 17% of day 1, whereas non-functionalized gels remained with 71% of initial area over time in culture.

Indeed, matrix contraction has already been described for different RGD-functionalized polymers [144,138,163] such as pectin hydrogels with similar shear moduli [138]. Indeed, as RGD peptides are known to bind integrins [164,165] and contractile forces exerted by cells in culture are transferred to the surrounding matrix through transcellular adhesions such as

these [166], the observed decrease in surface area might have been a result of matrix contraction triggered by this phenomenon. Moreover, as area variation was higher and noticeable earlier for formulations modified with higher RGD concentrations (2 mM), reaction with increased amounts of peptide might have resulted in an increase in number of functionalized moieties, leading to a higher number of cell adhesive sites and consequently higher matrix contraction.

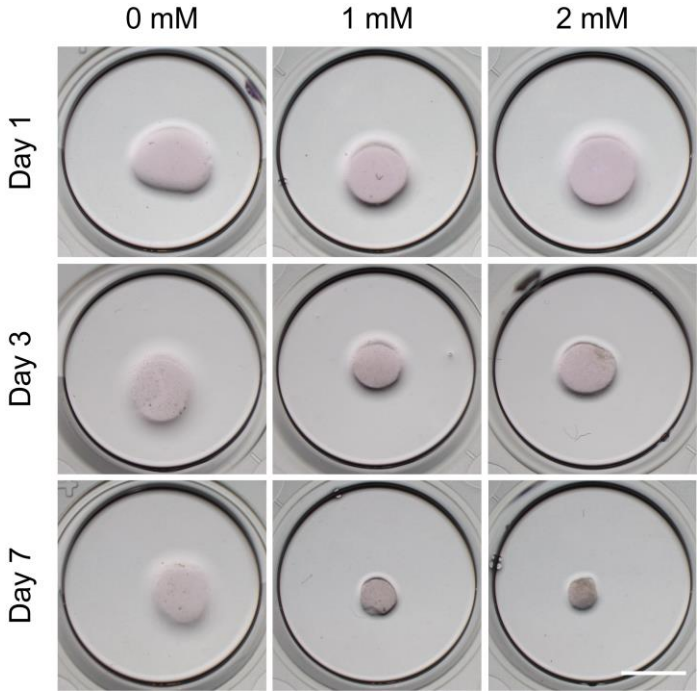

Figure 17: Macroscopic view of cell-laden HAMA/PectMA hydrogels with varying RGD content after 1, 3 and 7 days in culture. Scale bar = 5 mm.

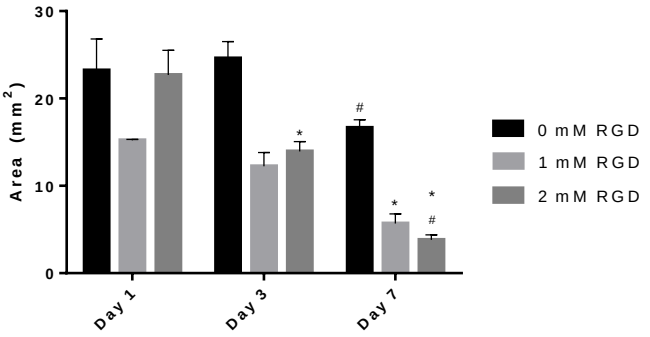

Figure 18: Influence of the incorporation of RGD peptide on disk area legend: symbols denote statistically significant differences ($p<0.05$) from day 1 (*), day 3 (#), n=3.

4.3.3. CELL METABOLIC ACTIVITY (RESAZURIN REDUCTION ASSAY)

HDNF metabolic activity was evaluated after 1, 3, and 7 days using the resazurin reduction assay and normalized for cell number within each hydrogel. After 1 day in culture, no differences were noticeable between cells cultured in hydrogels with varying concentrations of one of the polymers in the mixture while keeping the other constant. Differences between formulations at the same timepoint were only observed on day 3 for disks with different HAMA content. Here, cells encapsulated in hydrogels composed of 0.75% HAMA exhibited the highest values of metabolic activity, followed by the formulations with 1.5% HAMA. Cells encapsulated in 0.125% HAMA exhibited the lowest metabolic activity values. However, after 7 days, a significant decrease in metabolic activity was observed for all formulations when compared to values of day 1.

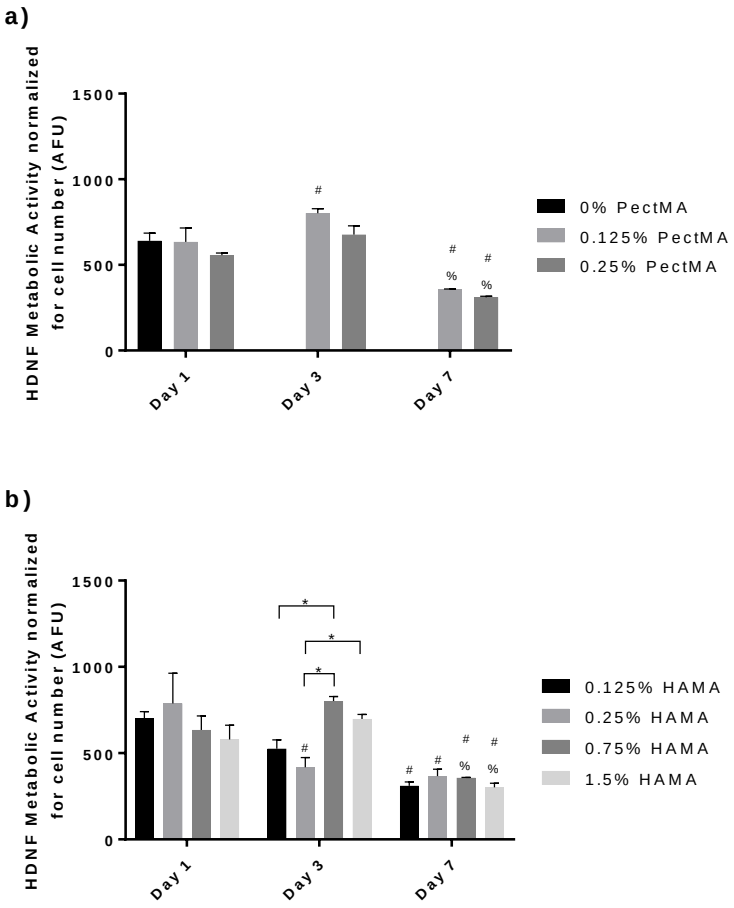

Figure 19: Metabolic activity of cells embedded in HAMA/PectMA hydrogels of (a) 0.125% PectMA, with varying %HAMA; (b) 0.75% HAMA, with varying %PectMA. Data for 0% PectMA formulations not shown as hydrogel disks lost integrity after 3 days in culture. Legend: symbols denote statistically significant differences ($p<0.05$) between different formulations (*), from day 1 (#), from day 3 (%), n=3.

For RGD-functionalized hydrogels, a similar behaviour to non-modified formulations was found, with cell metabolic activity decreasing with longer culture times, but with no significant differences among the three formulations studied (Figure 20). Indeed, a decrease in number of metabolically active cells has already been reported after fibroblast entrapment in RGD-functionalized hydrogels that occurred along with hydrogel matrix contraction after day 3 [163].

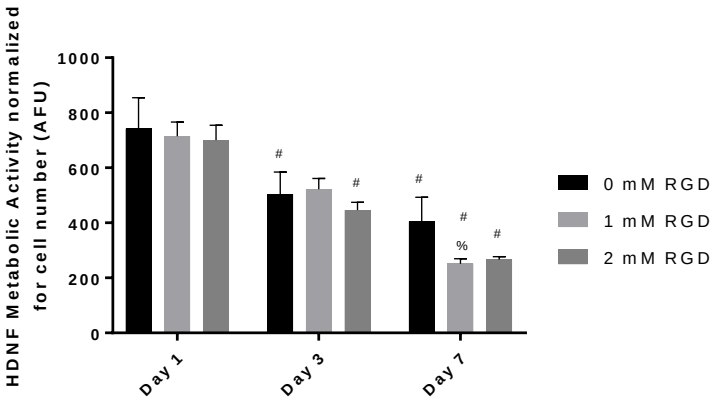

Figure 20: Metabolic activity of cells embedded in HAMA/PectMA hydrogels of 0.125% PectMA, 0.75% HAMA functionalized with RGD peptides. Legend: Symbols denote statistically significant differences ($p<0.05$) from day 1 (#), from day 3 (%), n=3.

4.3.4. Cell viability (Live/Dead assay)

Live/Dead evaluation of cells embedded in HAMA/PectMA hydrogels revealed that most cells remained viable over time in culture both for hydrogels containing varying PectMA (Figure 21) or HAMA (Figure 22) content. Hydrogels containing either 0% or 0.125% PectMA seem to lead to cell clustering on day 3 whereas for 0.25% PectMA that phenomenon is less noticeable and only starts to be apparent on day 7. Indeed, higher PectMA content leads to hydrogels with higher shear elastic moduli, possibly hindering cell mobility within the matrix. As polymers not functionalized with RGD were used herein, cells were not able to attach to the matrix and kept a rounded morphology throughout the 7 days in culture. As fibroblasts are adherent cells and hydrogels with lower PectMA content did not seem to limit cell mobility, cells were able to form clusters and possibly establish cell-cell adhesions, as an anchorage support within the hydrogel matrix. .

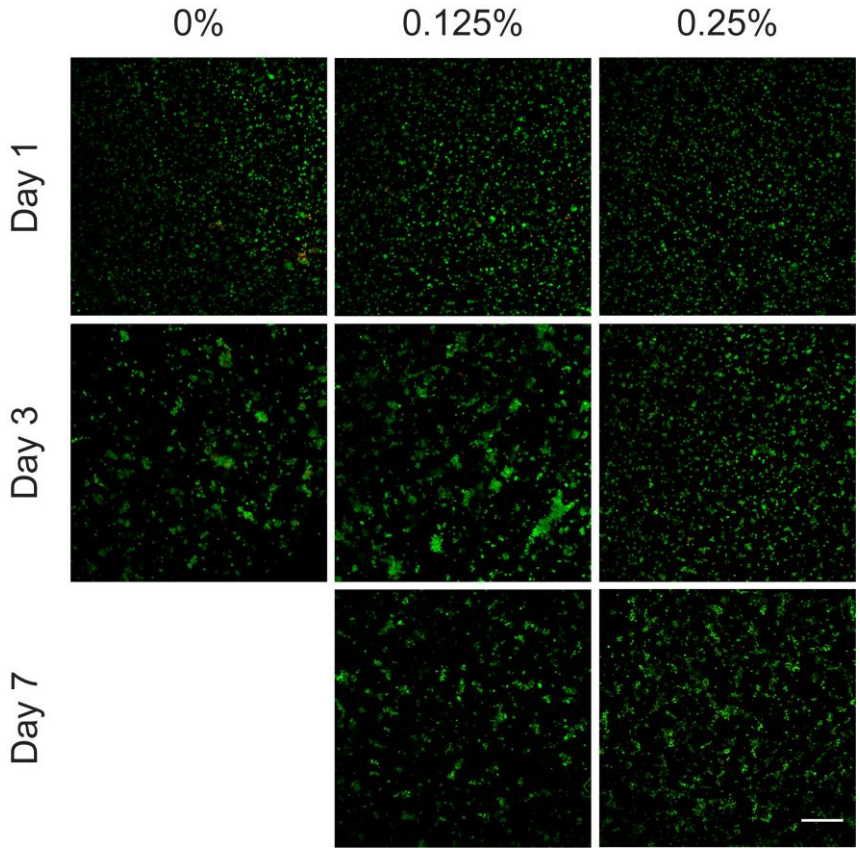

Figure 21: Viability of HDNFs cultured in HAMA/PectMA hydrogel disks for 1, 3 and 7 days with varying PectMA content. Live cells are stained green by Calcein AM and dead cells red by Propidium Iodide. 0% PectMA hydrogels not shown due to loss of integrity before day 7. Scale bar: 250 µm.

When increasing % HAMA, formulations with lower polymer content appeared to have a higher cell density (Figure 22), which might be due to the fact that these disks exhibited lower dimensions when compared with formulations with higher polymer content (Figure 16). Indeed, even though lower cell numbers were retrieved from gels with lower HAMA content (Figure 12), smaller dimensions might have been sufficient to lead to an apparently higher cell density. In addition, hydrogels with lower HAMA content seem to contain greater amounts of dead cells (stained red on Figure 22). These formulations contained very low polymer concentration that were possibly not optimal to sustain cells in culture for prolonged periods of time.

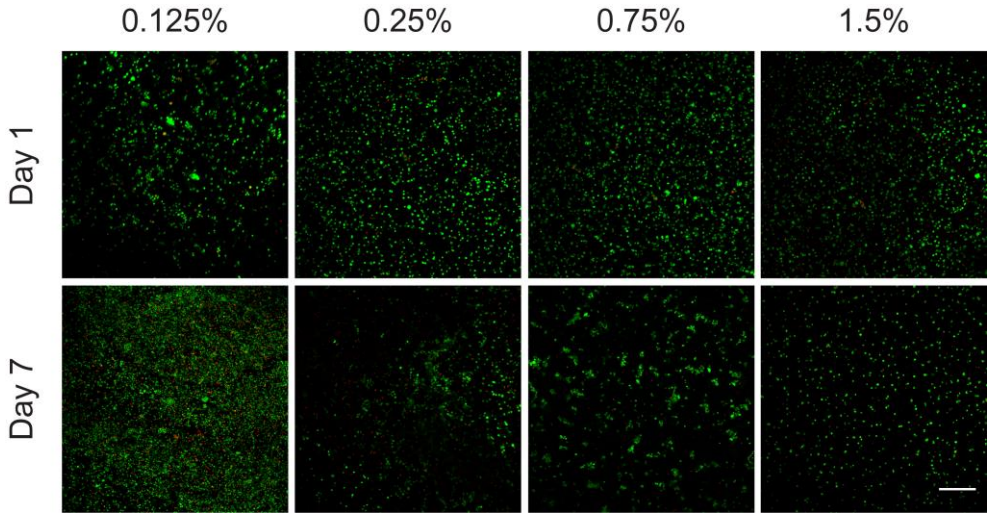

Figure 22: Viability of HDNFs cultured in HAMA/PectMA hydrogel disks for 1, 3 and 7 days with varying HAMA content. Live cells are stained green by calcein AM and dead cells red by propidium iodide. Scale bar: 250 µm.

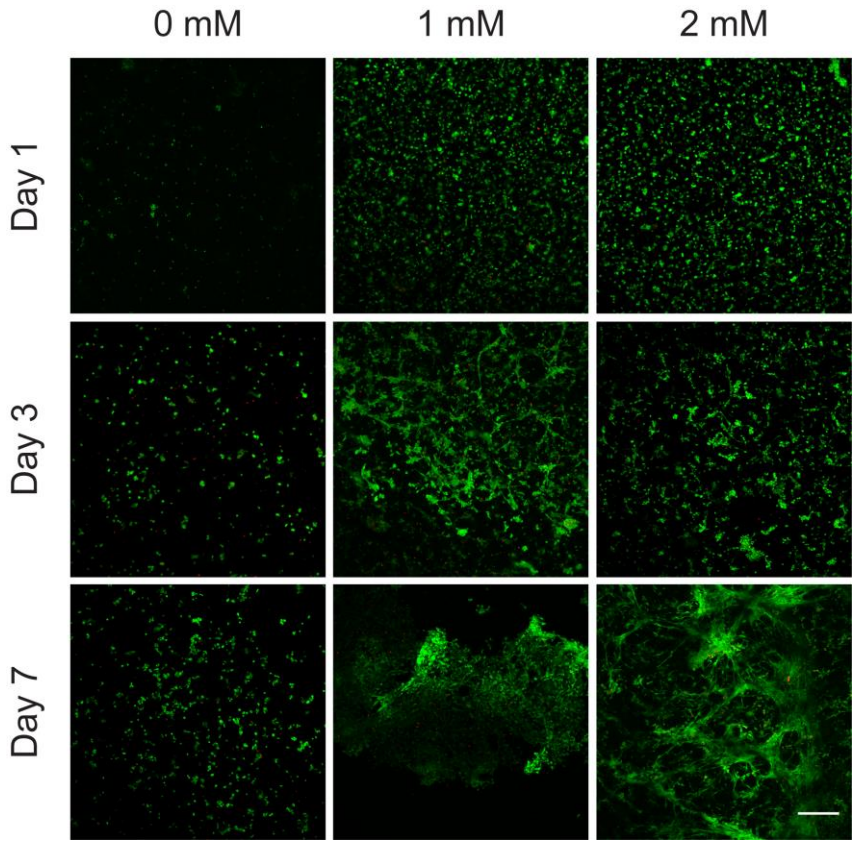

Figure 23: viability of HDNFs cultured in HAMA/PectMA hydrogel disks for 1, 3 and 7 days with varying RGD content. Live cells are stained green by calcein am and dead cells red by propidium iodide. Scale bar = 250 µm. Note: 1 mM day 7 micrograph pictures a fragment of the cultured hydrogel.

Hydrogel functionalization with RGD peptides resulted on similarly high cell viability for the three formulations, with the majority of cells staining green throughout the 7 days in culture, supporting that 0.75% HAMA / 0.125% PectMA hydrogels are able to maintain encapsulated cells with a high viability upon entrapment and over time in culture.

4.3.5. Cytoskeleton and matrix production (immunocytochemistry)

After being cultured for 1, 3, and 7 days, cells were stained for F-actin and fibronectin in order to evaluate cell morphology and cytoskeleton, and matrix deposition.

When cultured inside hydrogels containing 0.75% HAMA with increasing PectMA content, cells exhibited a round morphology on day 1, becoming slightly more elongated after 7 days in culture, particularly in hydrogels with 0.125% PectMA.

In addition, for hydrogels with low to no PectMA content (0% and 0.125%) and lower shear elastic moduli, cells appear to form clusters on day 3. However, for longer culture periods, disks composed of HAMA in the absence of PectMA (0%) lost their integrity before day 7, while disks containing PectMA (0.125%) kept their integrity. In this latter formulation, cells presented a more elongated morphology, which was less noticeable when PectMA content was doubled to 0.25% (Figure 24). Indeed, the presence of PectMA seemed to be necessary to keep the integrity of cell-loaded 0.75% HAMA hydrogels in culture over time and has a clear influence on cell morphology. Indeed, modification by reaction with MA generates photocrosslinkable pectin, which reticulates upon exposure to UV light. In addition, as pectin is known to be able to form hydrogels by internal [138] or external gelation [139], this polymer might still be able to coordinate Ca^{2+} ions after photopolymerization, providing cell-laden hydrogels with structural stability and preventing its disruption triggered by cells.

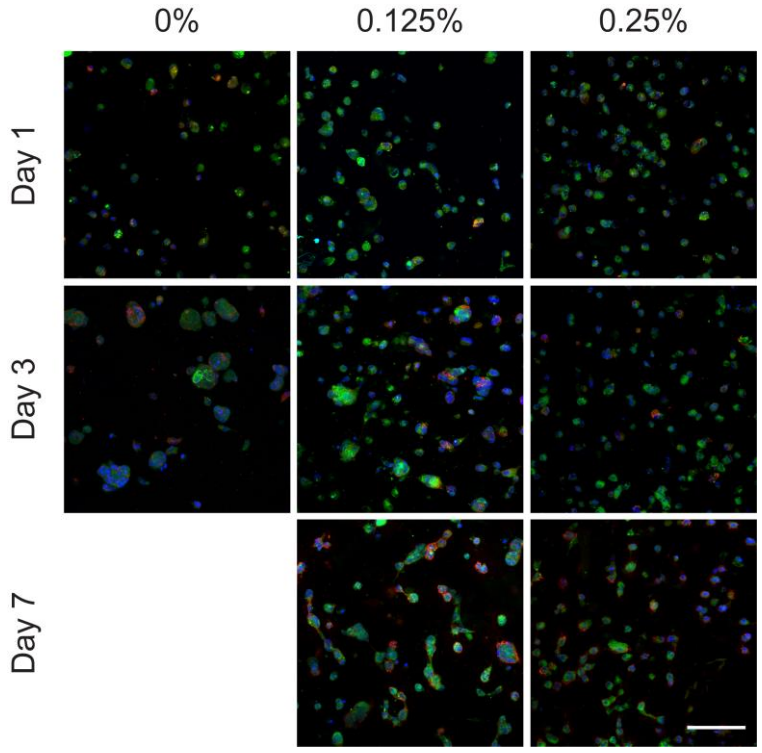

Figure 24: HDNFs embedded in HAMA/PectMA hydrogels with 0.75% HAMA and increasing % PectMA, stained for F-actin (green), fibronectin (red) and nuclei (blue). 0% PectMA hydrogels not shown due to loss of integrity before day 7. Scale bar: 100 µm.

Additionally, in order to evaluate the influence of HAMA, cell-laden hydrogels containing 0.125% PectMA and increasing HAMA content were fabricated (Figure 25). Disks produced with low HAMA content (0.125%) appear to promote an increase in cell density within the matrix, observable as a higher number of cells per area (Figure 25), possibly as a consequence of smaller disk dimensions, as macroscopically observed (Figure 14). Accordingly, increasing the HAMA content of hydrogels disks seems to lead to lower cell densities (Figure 25). Indeed, whereas hydrogels with different PectMA content exhibited similar dimensions in culture, increasing HAMA concentration resulted in the fabrication of hydrogel disks that appeared larger after 1 day (Figure 16), even though all disks were initially fabricated with the same volume of pre-polymer solution. Therefore, and due to the fact that cells were embedded in the hydrogels as a homogeneous suspension and no cell-adhesive motifs were present in the matrix, cells may have been further separated from each other within the network during the first day in culture as hyaluronic acid is able to absorb a high quantity of water as a result of the presence of negative charges [128].

Regarding fibronectin deposition, this protein was mostly located around cells, with no major differences being observed among the different formulations produced from non-functionalized pre-polymer solutions. These results suggest that neither PectMA nor HAMA

had a differential ability to modulate cell behaviour, with the hydrogels acting only as reservoir of cells.

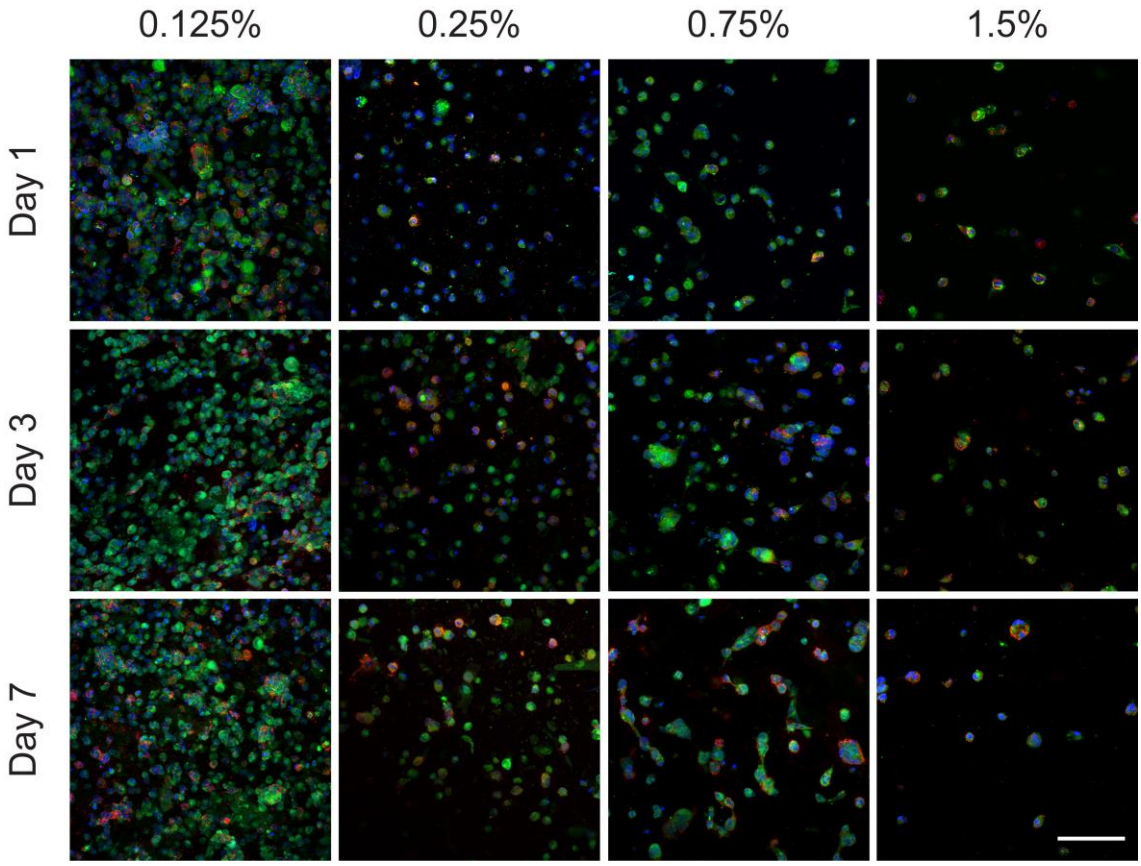

Figure 25: HDNFs embedded in HAMA/PectMA hydrogels with 0.125% PectMA and increasing % HAMA, stained for F-actin (green), fibronectin (red) and nuclei (blue). Scale bar: 100 µm.

As matrices composed of 0.75% HAMA / 0.125% PectMA enabled cells to move within the hydrogel and promoted slightly higher cell spreading when compared with the remaining formulations, hydrogels with this composition were further functionalized with RGD peptides, molecules known to promote integrin-mediated cell adhesion.

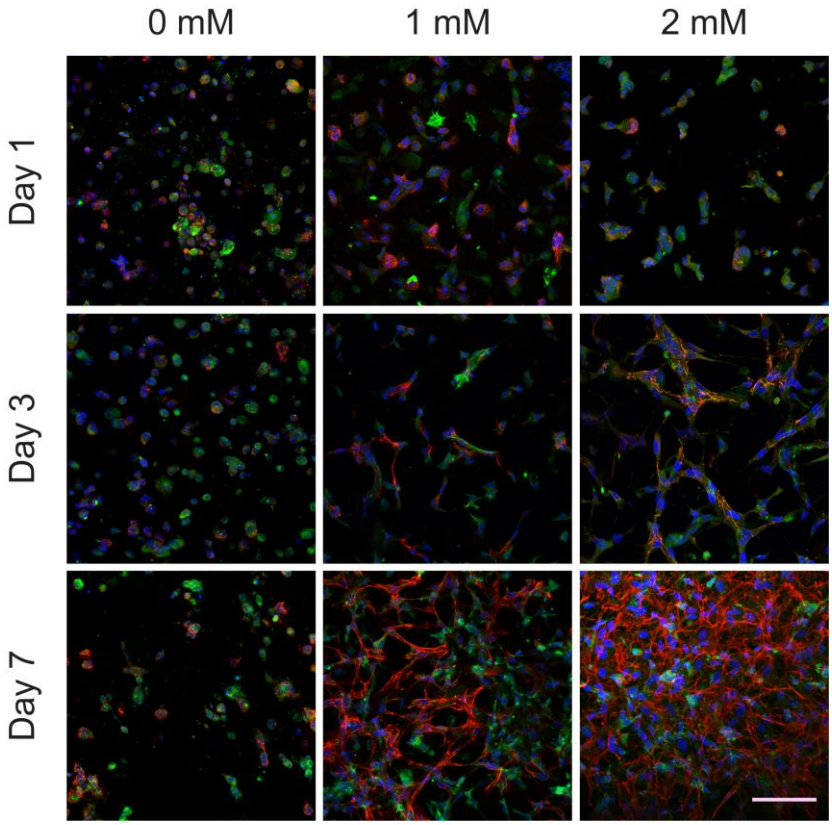

Figure 26: HDNFs embedded in HAMA/PectMA hydrogels with 0.125% PectMA, 0.75% HAMA and increasing RGD concentration, stained for F-actin (green), fibronectin (red) and nuclei (blue). Scale bar: 100 µm.

The modification of hydrogel matrices with RGD peptides led to an increased cell spreading, which was detected as soon as 1 day after entrapment for both 1 mM and 2 mM formulations and became more evident after 3 and 7 days. By this time, encapsulated cells appeared with a more spindle-shaped morphology, possibly establishing cell-cell contacts with time. Moreover, a network of fibronectin mostly located around cells was formed and appeared prominently on day 7. Indeed, fibronectin is an ECM protein known to be produced by fibroblasts [167] and was chosen herein as an example of matrix deposition. In addition, this fibronectin network appeared denser in 2 mM hydrogels when compared with 1 mM formulation, due to either increased fibronectin production or matrix contraction. Indeed, hydrogels containing 2 mM RGD suffered higher and earlier matrix contraction when compared to 0 and 1 mM formulations, as visible both macroscopically (Figure 17) and microscopically as a higher density of cell nuclei appeared prominently on 2 mM hydrogels on day 7 (Figure 26). Nevertheless, hydrogel functionalization with RGD peptides seemed to promote cell attachment to the matrix, with cells acquiring an elongated phenotype not very evident in non-functionalized matrices, as well as endogenous ECM production.

RGD peptides are well known promoters of cell adhesion and spreading [168], as they are recognized and bind several types of integrin such as α5β1 and αvβ3 [164]. The strength of cell adhesion to RGD-modified substrates has been shown to be higher for increased RGD densities [169]. Moreover, these peptides are also able to sustain cell migration, with higher cell speeds being observed for higher RGD ligand densities both in 2D [169] and 3D [156]. RGD motifs are present in a wide range of proteins such as fibronectin, vitronectin and laminins [164] and are commonly used in order to promote cell adhesion to polymers which would not elicit it otherwise [170]. Indeed, RGD-modifications have previously been conducted in both hyaluronic acid [154–156] and pectin [138,150], as both hyaluronic acid and pectin are unable to bind integrins [128].

In this work, hyaluronic acid and pectin were methacrylated and the resulting polymers were modified with RGD, generating hydrogel matrices with low shear moduli that are capable of promoting cell adhesion, matrix contraction and ECM production while keeping its integrity and high cell viability for up to 7 days in culture.

CHAPTER 5: CONCLUSIONS AND FUTURE PERSPECTIVES

This work aimed at fabricating soft, photopolymerizable hydrogels composed of HAMA and PectMA to be used as a skin *in vitro* model for a high-throughput skin organ-on-a-chip device. Using UV-induced free radical photopolymerization, hydrogel disks with tuneable shear moduli could be produced using different polymer concentrations and ratios. Hence, by increasing polymer content, hydrogels with higher moduli were fabricated. This was observed when increasing either HAMA or PectMA concentrations.

Furthermore, the biological performance of the developed hydrogels was herein assessed through the entrapment of human dermal neonatal fibroblasts. When cultured with cells, hydrogels fabricated with increasing PectMA content were able to sustain culture of HDNFs for up to 7 days. However, formulations composed only of 0.75% HAMA (0% PectMA) started losing their structural integrity after being cultured for 3 days, whereas the addition of a 0.125% PectMA was enough to keep the system stable while promoting a slightly more elongated cell morphology, visible at 7 days.

Overall, variations of HAMA content resulted in differences both in terms of hydrogel size in culture and of cell distribution and response. Higher polymer concentrations resulted in hydrogels with larger area, while increased cell densities were found in hydrogels with lower HAMA content. In particular, cell spreading was more evident in hydrogels composed of 0.75% HAMA, possibly due to an interplay between hydrogel swelling and mechanical properties of the matrix. Nonetheless, these hydrogels could only act as a reservoir of cells, given that HAMA and PectMA are relatively inert regarding cell adhesive cues. Therefore, RGD-functionalized hydrogels were fabricated and exhibited superior performance, allowing cells to interact with the hydrogel matrix, which, in turn, led to a contraction of the disks. This phenomenon was dependent on RGD concentrations, happening earlier for formulations with higher RGD content. In these matrices, cells appeared elongated and spindle-shaped and a fibronectin network which was denser for hydrogels with higher RGD content was formed and visible after 7 days in culture. Nevertheless, further characterization of RGD functionalization reaction and efficiency is still needed to fully understand the system.

In summary, a two-polymer hydrogel system was produced and characterized both in terms of mechanical and cellular behaviour. The use of a dual system allowed to independently vary polymer concentrations and ratios, resulting in tuneable mechanical and biological properties while keeping shear moduli low and producing soft hydrogels. However, future studies are still

necessary in order to evaluate cell culture for longer periods of time and further characterize the resulting cellularized constructs.

Furthermore, the recapitulation of functionally similar to human skin in terms of transdermal transport, wound healing and toxicity response constitutes a major challenge to address when engineering *in vitro* skin constructs to be suitable for a skin-on-chip device. Overall, this work provided meaningful insight into the mechanical and biological behaviour of a novel photopolymerizable two-polymer hydrogel system with potential impact on the development of novel high-throughput skin emulative strategies using 3D bioprinting.

REFERENCES

[1] P.G. Agache, P. Agache, P. Humbert, Measuring the Skin, Springer, 2004. https://books.google.pt/books?id=APiLX8aBakkC.

[2] A.D. Metcalfe, M.W.J. Ferguson, Tissue engineering of replacement skin: the crossroads of biomaterials, wound healing, embryonic development, stem cells and regeneration, J. R. Soc. Interface. 4 (2007) 413–437. doi:10.1098/rsif.2006.0179.

[3] K.C. Madison, Barrier Function of the Skin: "'La Raison d'EOE tre"' of the Epidermis, J. Invest. Dermatol. 121 (2003) 231–241. doi:10.1046/j.1523-1747.2003.12359.x.

[4] D.A. Barrett, N. Rutter, Transdermal delivery and the premature neonate., Crit. Rev. Ther. Drug Carrier Syst. 11 (1994) 1–30.

[5] P. Arora, B. Mukherjee, Design, development, physicochemical, and in vitro and in vivo evaluation of transdermal patches containing diclofenac diethylammonium salt, J. Pharm. Sci. 91 (2002) 2076–2089. doi:10.1002/jps.10200.

[6] M.R. Prausnitz, R. Langer, Transdermal drug delivery, Nat. Biotechnol. 26 (2008) 1261–1268. doi:10.1038/nbt.1504.

[7] P. Karande, A. Jain, S. Mitragotri, Discovery of transdermal penetration enhancers by high-throughput screening., Nat. Biotechnol. 22 (2004) 192–197. doi:10.1038/nbt928.

[8] C.K. Sen, G.M. Gordillo, S. Roy, R. Kirsner, L. Lambert, T.K. Hunt, et al., Human skin wounds: A major and snowballing threat to public health and the economy, Wound Repair Regen. 17 (2009) 763–771. doi:10.1111/j.1524-475X.2009.00543.x.

[9] United Nations, Globally Harmonized System of Classification and Labelling of Chemicals (Ghs), 2011.

[10] OECD, OECD Guidelines For the Testing of Chemicals. 439. In Vitro Skin Irritation: Reconstructed Human Epidermis Test Method, (2015) 1–21.

[11] OECD, OECD Guideline for the testing of chemicals. 442D. In Vitro Skin Sensitisation : ARE-Nrf2 Luciferase Test Method, (2015).

[12] OECD, OECD Guidelines For the Testing of Chemicals. 431. In vitro skin corrosion: reconstructed human epidermis (RHE) test method, (2015).

[13] OECD, OECD guidlines for the testing of chemicals. 428. Skin Absorption: in vitro Method, (2004).

[14] R.F. Pereira, C.C. Barrias, P.L. Granja, P.J. Bartolo, Advanced biofabrication strategies for skin regeneration and repair., Nanomedicine (Lond). 8 (2013) 603–21. doi:10.2217/nnm.13.50.

[15] E.W. Esch, A. Bahinski, D. Huh, Organs-on-chips at the frontiers of drug discovery., Nat. Rev. Drug Discov. 14 (2015) 248–260. doi:10.1038/nrd4539.

[16] S.N. Bhatia, D.E. Ingber, Microfluidic organs-on-chips, Nat. Biotechnol. 32 (2014) 760–772. doi:10.1038/nbt.2989.

[17] N. Alépée, N. Alepee, A. Bahinski, M. Daneshian, B. De Wever, E. Fritsche, et al., State-of-the-art of 3D cultures (organs-on-a-chip) in safety testing and pathophysiology, ALTEX. 31 (2014) 441–77. doi:10.14573/altex1406111.

[18] European Commission, REGULATION (EC) No 1223/2009 OF THE EUROPEAN PARLIAMENT AND OF THE COUNCIL, Off. J. Eur. Union. (2009) 342/59-208.

[19] M.R. Prausnitz, S. Mitragotri, R. Langer, Current status and future potential of transdermal drug delivery, Nat. Rev. Discov. 3 (2004) 115–124. doi:10.1038/nrd1304.

[20] Scientific Committee on Consumer Safety, Basic criteria for the in vitro assessment of dermal absorption of cosmetic ingredients, Eur. Comm. SCCS/1358 (2010) 1–14. doi:10.2772/25843.

[21] A. Naegel, M. Heisig, G. Wittum, Detailed modeling of skin penetration-An overview, Adv. Drug Deliv. Rev. 65 (2013) 191–207. doi:10.1016/j.addr.2012.10.009.

[22] H.F. Frasch, A.M. Barbero, Application of numerical methods for diffusion-based

modeling of skin permeation, Adv. Drug Deliv. Rev. 65 (2013) 208–220. doi:10.1016/j.addr.2012.01.001.
[23] OECD, OECD guidlines for the testing of chemicals. 427. Skin absorption: in vivo method, (2004) 1–8. doi:10.1787/9789264071063-en.
[24] OECD, Guidance Document for the Conduct of Skin Absorption Studies, OECD Publishing, 2004. doi:10.1787/9789264078796-en.
[25] M.J. Bartek, J. a LaBudde, H.I. Maibach, Skin permeability in vivo: comparison in rat, rabbit, pig and man., J. Invest. Dermatol. 58 (1972) 114–123. doi:10.1111/1523-1747.ep12538909.
[26] W.G. Reifenrath, E.M. Chellquist, E. a Shipwash, W.W. Jederberg, G.G. Krueger, Percutaneous penetration in the hairless dog, weanling pig and grafted athymic nude mouse: evaluation of models for predicting skin penetration in man., Br. J. Dermatol. 111 Suppl (1984) 123–35. http://www.ncbi.nlm.nih.gov/pubmed/6204672.
[27] T. Winsor, G.E. Burch, Differential roles of layers of human epigastric skin on diffusion rate of water, Arch. Intern. Med. 74 (1944) 428. doi:10.1001/archinte.1944.00210240018004.
[28] E. Fuchs, H. Green, Changes in keratin gene expression during terminal differentiation of the keratinocyte., Cell. 19 (1980) 1033–1042. doi:10.1016/0092-8674(80)90094-X.
[29] P.M. Elias, Epidermal lipids, barrier function, and desquamation., J. Invest. Dermatol. 80 Suppl (1983) 44s–49s. doi:10.1111/1523-1747.ep12537108.
[30] M.R. Prausnitz, P.M. Elias, T.J. Franz, M. Schmuth, J. Tsai, G.K. Menon, et al., Skin Barrier and Transdermal Drug Delivery, Dermatology. (2012) 2065–2073. doi:10.1016/B978-0-7234-3571-6.00124-X.
[31] S. Grayson, P.M. Elias, Isolation and Lipid Biochemical Characterization of Stratum Corneum Membrane Complexes: Implications for the Cutaneous Permeability Barrier., J. Invest. Dermatol. 78 (1982) 128–135. doi:10.1111/1523-1747.ep12505953.
[32] G. Imokawa, M. Hattori, A Possible Function of Structural Lipids in the Water-Holding Properties of the Stratum Corneum., J. Invest. Dermatol. 84 (1985) 282–284. doi:10.1111/1523-1747.ep12265365.
[33] G. Imokawa, H. Kuno, M. Kawai, Stratum corneum lipids serve as a bound-water modulator., J. Invest. Dermatol. 96 (1991) 845–851. doi:10.1111/1523-1747.ep12474562.
[34] E. Berardesca, F. Distante, G.P. Vignoli, C. Oresajo, B. Green, Alpha hydroxyacids modulate stratum corneum barrier function., Br. J. Dermatol. 137 (1997) 934–938. doi:10.1046/j.1365-2133.1997.19882069.x.
[35] E. Boireau-Adamezyk, A. Baillet-Guffroy, G.N. Stamatas, Age-dependent changes in stratum corneum barrier function, Ski. Res. Technol. 20 (2014) 409–415. doi:10.1111/srt.12132.
[36] G. Yosipovitch, G.L. Xiong, E. Haus, L. Sackett-Lundeen, I. Ashkenazi, H.I. Maibach, Time-dependent variations of the skin barrier function in humans: transepidermal water loss, stratum corneum hydration, skin surface pH, and skin temperature., J. Invest. Dermatol. 110 (1998) 20–3. doi:10.1046/j.1523-1747.1998.00069.x.
[37] J.-P. Hachem, D. Crumrine, J. Fluhr, B.E. Brown, K.R. Feingold, P.M. Elias, pH directly regulates epidermal permeability barrier homeostasis, and stratum corneum integrity/cohesion., J. Invest. Dermatol. 121 (2003) 345–53. doi:10.1046/j.1523-1747.2003.12365.x.
[38] R.H. Wildnauer, J.W. Bothwell, A.B. Douglass, Stratum Corneum Biomechanical Properties I. Influence of Relative Humidity on Normal and Extracted Human Stratum Corneum., J. Invest. Dermatol. 56 (1971) 72–78. doi:10.1111/1523-1747.ep12292018.
[39] G.M. Golden, D.B. Guzek, a H. Kennedy, J.E. McKie, R.O. Potts, Stratum corneum lipid phase transitions and water barrier properties., Biochemistry. 26 (1987) 2382–8. doi:10.1021/bi00382a045.

[40] G.M. Golden, J.E. McKie, R.O. Potts, Role of stratum corneum lipid fluidity in transdermal drug flux., J. Pharm. Sci. 76 (1987) 25–28. doi:10.1002/jps.2600760108.
[41] S.N. Andrews, E. Jeong, M.R. Prausnitz, Transdermal delivery of molecules is limited by full epidermis, not just stratum corneum, Pharm. Res. 30 (2013) 1099–1109. doi:10.1007/s11095-012-0946-7.
[42] S. Gibbs, J.J.M. van de Sandt, H.F. Merk, D.J. Lockley, R.U. Pendlington, C.K. Pease, Xenobiotic metabolism in human skin and 3D human skin reconstructs: a review, Curr. Drug Metab. 8 (2007) 758–772. doi:10.2174/138920007782798225.
[43] C.K. Svensson, Biotransformation of Drugs in Human Skin, Drug Metab. Dispos. 37 (2009) 247–253. doi:10.1124/dmd.108.024794.nel.
[44] D. Zalko, C. Jacques, H. Duplan, S. Bruel, E. Perdu, Viable skin efficiently absorbs and metabolizes bisphenol A., Chemosphere. 82 (2011) 424–30. doi:10.1016/j.chemosphere.2010.09.058.
[45] B.W. Barry, Novel mechanisms and devices to enable successful transdermal drug delivery, Eur. J. Pharm. Sci. 14 (2001) 101–114. doi:10.1016/S0928-0987(01)00167-1.
[46] P. Karande, S. Mitragotri, High throughput screening of transdermal formulations, Pharm. Res. 19 (2002) 655–660. doi:10.1023/A:1015362230726.
[47] S. Andega, N. Kanikkannan, M. Singh, Comparison of the effect of fatty alcohols on the permeation of melatonin between porcine and human skin, J. Control. Release. 77 (2001) 17–25. doi:10.1016/S0168-3659(01)00439-4.
[48] A. Kogan, N. Garti, Microemulsions as transdermal drug delivery vehicles, Adv. Colloid Interface Sci. 123–126 (2006) 369–385. doi:10.1016/j.cis.2006.05.014.
[49] N.B. Smith, S. Lee, E. Maione, R.B. Roy, S. McElligott, K.K. Shung, Ultrasound-mediated transdermal transport of insulin in vitro through human skin using novel transducer designs, Ultrasound Med. Biol. 29 (2003) 311–317. doi:10.1016/S0301-5629(02)00706-8.
[50] S. Henry, D. V McAllister, M.G. Allen, M.R. Prausnitz, Microfabricated microneedles: A novel approach to transdermal drug delivery, J. Pharm. Sci. 87 (1998) 922–925. doi:10.1021/js980042+.
[51] A. Tezel, A. Sens, J. Tuchscherer, S. Mitragotri, Synergistic effect of low-frequency ultrasound and surfactants on skin permeability, J. Pharm. Sci. 91 (2002) 91–100. doi:10.1002/jps.10000.
[52] R.C. Wester, X. Hui, T. Hartway, H.I. Maibach, K. Bell, M.J. Schell, et al., In vivo percutaneous absorption of boric acid, borax, and disodium octaborate tetrahydrate in humans compared to in vitro absorption in human skin from infinite and finite doses, Toxicol. Sci. 45 (1998) 42–51. doi:10.1006/toxs.1998.2490.
[53] R. Elkeeb, X. Hui, H. Chan, L. Tian, H.I. Maibach, Correlation of transepidermal water loss with skin barrier properties in vitro: comparison of three evaporimeters., Skin Res. Technol. 16 (2010) 9–15. doi:10.1111/j.1600-0846.2009.00406.x.
[54] D.J. Davies, R.J. Ward, J.R. Heylings, Multi-species assessment of electrical resistance as a skin integrity marker for in vitro percutaneous absorption studies, Toxicol. Vitr. 18 (2004) 351–358. doi:10.1016/j.tiv.2003.10.004.
[55] R.E. Imhof, E.P. Berg, R.P. Chilcott, L.I. Ciortea, F.C. Pascut, P. Xiao, New Instrument for Measuring Water Vapor Flux Density from Arbitrary Surfaces, Ifscc. 5 (2002) 297–301. file://g/Library/Reference Manager/Papers/877. IFSCC, 2002, 5(4),. 297-301.pdf.
[56] E. Elmahjoubi, Y. Frum, G.M. Eccleston, S.C. Wilkinson, V.M. Meidan, Transepidermal water loss for probing full-thickness skin barrier function: correlation with tritiated water flux, sensitivity to punctures and diverse surfactant exposures., Toxicol. In Vitro. 23 (2009) 1429–35. doi:10.1016/j.tiv.2009.06.030.
[57] T. Byford, Environmental Health Criteria 235: Dermal Absorption, Int. J. Environ. Stud. 66 (2009) 662–663. doi:10.1080/00207230802361240.
[58] D.R. Friend, In vitro skin permeation techniques, J. Control. Release. 18 (1992) 235–248.

doi:10.1016/0168-3659(92)90169-R.
[59] J. Kao, F.K. Patterson, J. Hall, Skin penetration and metabolism of topically applied chemicals in six mammalian species, including man: an in vitro study with benzo[a]pyrene and testosterone., Toxicol. Appl. Pharmacol. 81 (1985) 502–516. doi:10.1016/0041-008X(85)90421-1.
[60] S.M. Harrison, B.W. Barry, P.H. Dugard, Effects of freezing on human skin permeability., J. Pharm. Pharmacol. 36 (1984) 261–2. doi:10.1111/j.2042-7158.1984.tb04363.x.
[61] A.L. Stinchcomb, P.W. Swaan, O. Ekabo, K.K. Harris, J. Browe, D.C. Hammell, et al., Straight-chain naltrexone ester prodrugs: diffusion and concurrent esterase biotransformation in human skin., J. Pharm. Sci. 91 (2002) 2571–8. doi:10.1002/jps.10239.
[62] F.P. Schmook, J.G. Meingassner, A. Billich, Comparison of human skin or epidermis models with human and animal skin in in-vitro percutaneous absorption, Int. J. Pharm. 215 (2001) 51–56. doi:10.1016/S0378-5173(00)00665-7.
[63] I.P. Dick, R.C. Scott, Pig ear skin as an in-vitro model for human skin permeability., J. Pharm. Pharmacol. 44 (1992) 640–645. doi:10.1111/j.2042-7158.1992.tb05485.x.
[64] W.R. Galey, H.K. Lonsdale, S. Nacht, The in vitro permeability of skin and buccal mucosa to selected drugs and tritiated water., J. Invest. Dermatol. 67 (1976) 713–7. http://www.ncbi.nlm.nih.gov/pubmed/1033956.
[65] R.C. Scott, M. Walker, P.H. Dugard, A comparison of the in vitro permeability properties of human and some laboratory animal skins., Int. J. Cosmet. Sci. 8 (1986) 189–94. doi:10.1111/j.1467-2494.1986.tb00446.x.
[66] M. Schäfer-Korting, A. Mahmoud, S.L. Borgia, B. Brüggener, B. Kleuser, S. Schreiber, et al., Reconstructed epidermis and full-thickness skin for absorption testing: Influence of the vehicles used on steroid permeation, ATLA Altern. to Lab. Anim. 36 (2008) 441–452.
[67] S. Trauer, A. Patzelt, N. Otberg, F. Knorr, C. Rozycki, G. Balizs, et al., Permeation of topically applied caffeine through human skin - a comparison of *in vivo* and *in vitro* data, Br. J. Clin. Pharmacol. 68 (2009) 181–186. doi:10.1111/j.1365-2125.2009.03463.x.
[68] T.J. Franz, Percutaneous absorption on the relevance of in vitro data., J. Invest. Dermatol. 64 (1975) 190–195. doi:10.1111/1523-1747.ep12533356.
[69] S. Mitragotri, D. Blankschtein, R. Langer, Ultrasound-mediated transdermal protein delivery., Science. 269 (1995) 850–853. doi:10.1126/science.7638603.
[70] D. Mohammed, P.J. Matts, J. Hadgraft, M.E. Lane, In Vitro–In Vivo Correlation in Skin Permeation, Pharm. Res. 31 (2014) 394–400. doi:10.1007/s11095-013-1169-2.
[71] R.L. Bronaugh, R.F. Stewart, Methods for in vitro percutaneous absorption studies V: Permeation through damaged skin., J. Pharm. Sci. 74 (1985) 1062–1066.
[72] J.-M. Andanson, K.L.A. Chan, S.G. Kazarian, High-throughput spectroscopic imaging applied to permeation through the skin., Appl. Spectrosc. 63 (2009) 512–7. doi:10.1366/000370209788347011.
[73] P. Karande, S. Mitragotri, Dependence of skin permeability on contact area, Pharm. Res. 20 (2003) 257–263. doi:10.1023/A:1022231406277.
[74] G.S. Lazarus, D.M. Cooper, D.R. Knighton, D.J. Margolis, R.E. Pecoraro, G. Rodeheaver, et al., Definitions and guidelines for assessment of wounds and evaluation of healing., Arch. Dermatol. 130 (1994) 489–493. doi:10.1001/archderm.1994.01690040093015.
[75] V. Falanga, Wound healing and its impairment in the diabetic foot, Lancet. (2005). doi:10.1016/S0140-6736(05)67700-8.
[76] G.C. Gurtner, S. Werner, Y. Barrandon, M.T. Longaker, Wound repair and regeneration, Nature. 453 (2008) 314–321. doi:10.1038/nature07039.
[77] J. Li, J. Chen, R. Kirsner, Pathophysiology of acute wound healing, Clin. Dermatol. 25 (2007) 9–18. doi:10.1016/j.clindermatol.2006.09.007.
[78] P. Martin, Wound Healing--Aiming for Perfect Skin Regeneration, Science (80-.). 276 (1997) 75–81. doi:10.1126/science.276.5309.75.

[79] Raja, K. Sivamani, M.S. Garcia, R.R. Isseroff, Wound re-epithelialization: modulating keratinocyte migration in wound healing, Front. Biosci. 12 (2007) 2849—2868. doi:10.2741/2277.
[80] M. Zhao, Electrical fields in wound healing—An overriding signal that directs cell migration, Semin. Cell Dev. Biol. 20 (2009) 674–682. doi:10.1016/j.semcdb.2008.12.009.
[81] M.P. Rodero, K. Khosrotehrani, Skin wound healing modulation by macrophages, Int J Clin Exp Pathol. 3 (2010) 643–653.
[82] M.W. Carlson, A. Alt-Holland, C. Egles, J. a. Garlick, Three-dimensional tissue models of normal and diseased skin, Curr. Protoc. Cell Biol. (2008) 1–17. doi:10.1002/0471143030.cb1909s41.
[83] C.-C. Liang, A.Y. Park, J.-L. Guan, In vitro scratch assay: a convenient and inexpensive method for analysis of cell migration in vitro., Nat. Protoc. 2 (2007) 329–33. doi:10.1038/nprot.2007.30.
[84] B. Song, Y. Gu, J. Pu, B. Reid, Z. Zhao, M. Zhao, Application of direct current electric fields to cells and tissues in vitro and modulation of wound electric field in vivo, Nat. Protoc. 2 (2007) 1479–1489. doi:10.1038/nprot.2007.205.
[85] S. Song, H. Han, U.H. Ko, J. Kim, J.H. Shin, Collaborative effects of electric field and fluid shear stress on fibroblast migration., Lab Chip. 13 (2013) 1602–11. doi:10.1039/c3lc41240g.
[86] A.M. Das, A.M.M. Eggermont, T.L.M. Ten Hagen, A ring barrier-based migration assay to assess cell migration in vitro., Nat. Protoc. 10 (2015) 904–15. doi:10.1038/nprot.2015.056.
[87] S. Boyden, The Chemotactic Effect of Mixtures of Antibody and Antigen on Polymorphonuclear Leucocytes, Assessment. (1962) 453–466.
[88] H. Seppä, G. Grotendorst, S. Seppä, E. Schiffmann, G.R. Martin, Platelet-derived growth factor in chemotactic for fibroblasts., J. Cell Biol. 92 (1982) 584–8. doi:10.1083/jcb.92.2.584.
[89] T. Kohyama, R.F. Ertl, V. Valenti, J. Spurzem, M. Kawamoto, Y. Nakamura, et al., Prostaglandin E(2) inhibits fibroblast chemotaxis., Am. J. Physiol. Lung Cell. Mol. Physiol. 281 (2001) L1257–L1263.
[90] V. Falanga, C. Isaacs, D. Paquette, G. Downing, N. Kouttab, J. Butmarc, et al., Wounding of bioengineered skin: cellular and molecular aspects after injury., J. Invest. Dermatol. 119 (2002) 653–60. doi:10.1046/j.1523-1747.2002.01865.x.
[91] A. El Ghalbzouri, P. Hensbergen, S. Gibbs, J. Kempenaar, R. van der Schors, M. Ponec, Fibroblasts facilitate re-epithelialization in wounded human skin equivalents, Lab. Investig. 84 (2004) 102–112. doi:10.1038/labinvest.3700014.
[92] S. Küchler, N.B. Wolf, S. Heilmann, G. Weindl, J. Helfmann, M.M. Yahya, et al., 3D-wound healing model: influence of morphine and solid lipid nanoparticles., J. Biotechnol. 148 (2010) 24–30. doi:10.1016/j.jbiotec.2010.01.001.
[93] J.C. Yarrow, Z.E. Perlman, N.J. Westwood, T.J. Mitchison, A high-throughput cell migration assay using scratch wound healing, a comparison of image-based readout methods., BMC Biotechnol. 4 (2004) 21. doi:10.1186/1472-6750-4-21.
[94] V. Mastyugin, E. McWhinnie, M. Labow, F. Buxton, A quantitative high-throughput endothelial cell migration assay., J. Biomol. Screen. 9 (2004) 712–718. doi:10.1177/1087057104269495.
[95] F.-Q. Nie, M. Yamada, J. Kobayashi, M. Yamato, A. Kikuchi, T. Okano, On-chip cell migration assay using microfluidic channels., Biomaterials. 28 (2007) 4017–4022. doi:10.1016/j.biomaterials.2007.05.037.
[96] M.D. Zordan, C.P. Mill, D.J. Riese, J.F. Leary, A high throughput, interactive imaging, bright-field wound healing assay., Cytometry. A. 79 (2011) 227–32. doi:10.1002/cyto.a.21029.

[97] OECD, OECD Guideline for the Testing of Chemicals. 430. In Vitro Skin Corrosion: Transcutaneous Electrical Resistance Test Method (TER), (2015) 1–15.
[98] OECD, OECD Guidelines For the Testing of Chemicals. 435. In Vitro Membrane Barrier Test Method for Skin Corrosion, (2006) 1–15.
[99] E.L. Dahl, R. Curren, B.C. Barnett, Z. Khambatta, K. Reisinger, G. Ouedraogo, et al., The reconstructed skin micronucleus assay (RSMN) in EpiDerm (TM): Detailed protocol and harmonized scoring atlas, Mutat. Res. Toxicol. Environ. Mutagen. 720 (2011) 42–52. doi:10.1016/j.mrgentox.2010.12.001.
[100] OECD, OECD Guideline for the Testing of Chemicals. 487. In-vitro mammalian cell micronucleus test, OECD Guidel. (2014) 1–26.
[101] OECD, New Guidance Document on an Integrated Approach on Testing and Assessment (IATA) for Corrosion and Irritation, 33 (2009) 1–16. http://www.oecd.org/officialdocuments/displaydocumentpdf?cote=env/jm/mono(2010)46&doclanguage=en.
[102] R. Hamid, Y. Rotshteyn, L. Rabadi, R. Parikh, P. Bullock, Comparison of alamar blue and MTT assays for high through-put screening, Toxicol. Vitr. 18 (2004) 703–710. doi:10.1016/j.tiv.2004.03.012.
[103] A. Natsch, R. Emter, H. Gfeller, T. Haupt, G. Ellis, Predicting Skin Sensitizer Potency Based on In Vitro Data from KeratinoSens and Kinetic Peptide Binding: Global Versus Domain-Based Assessment, Toxicol. Sci. 143 (2014) 319–332. doi:10.1093/toxsci/kfu229.
[104] C. Bauch, S.N. Kolle, T. Ramirez, T. Eltze, E. Fabian, A. Mehling, et al., Putting the parts together: Combining in vitro methods to test for skin sensitizing potentials, Regul. Toxicol. Pharmacol. 63 (2012) 489–504. doi:10.1016/j.yrtph.2012.05.013.
[105] A. Natsch, R. Emter, G. Ellis, Filling the Concept with Data: Integrating Data from Different In Vitro and In Silico Assays on Skin Sensitizers to Explore the Battery Approach for Animal-Free Skin Sensitization Testing, Toxicol. Sci. 107 (2008) 106–121. doi:10.1093/toxsci/kfn204.
[106] D. Huh, B.D. Matthews, A. Mammoto, M. Montoya-Zavala, H.Y. Hsin, D.E. Ingber, Reconstituting Organ-Level Lung Functions on a Chip, Science (80-.). 328 (2010) 1662–1668. doi:10.1126/science.1188302.
[107] H.J. Kim, H. Li, J.J. Collins, D.E. Ingber, Contributions of microbiome and mechanical deformation to intestinal bacterial overgrowth and inflammation in a human gut-on-a-chip, Proc. Natl. Acad. Sci. (2015) 201522193. doi:10.1073/pnas.1522193112.
[108] K.-J. Jang, K.-Y. Suh, A multi-layer microfluidic device for efficient culture and analysis of renal tubular cells, Lab Chip. 10 (2010) 36–42. doi:10.1039/B907515A.
[109] K.-J. Jang, A.P. Mehr, G.A. Hamilton, L.A. McPartlin, S. Chung, K.-Y. Suh, et al., Human kidney proximal tubule-on-a-chip for drug transport and nephrotoxicity assessment, Integr. Biol. 5 (2013) 1119. doi:10.1039/c3ib40049b.
[110] P.J. Lee, P.J. Hung, L.P. Lee, An artificial liver sinusoid with a microfluidic endothelial-like barrier for primary hepatocyte culture, Biotechnol. Bioeng. 97 (2007) 1340–1346. doi:10.1002/bit.21360.
[111] Y. Torisawa, C.S. Spina, T. Mammoto, A. Mammoto, J.C. Weaver, T. Tat, et al., Bone marrow-on-a-chip replicates hematopoietic niche physiology in vitro., Nat. Methods. 11 (2014) 663–9. doi:10.1038/nmeth.2938.
[112] H.J. Kim, D. Huh, G. Hamilton, D.E. Ingber, Human gut-on-a-chip inhabited by microbial flora that experiences intestinal peristalsis-like motions and flow, Lab Chip. 12 (2012) 2165. doi:10.1039/c2lc40074j.
[113] H.E. Abaci, K. Gledhill, Z. Guo, A.M. Christiano, M.L. Shuler, Pumpless microfluidic platform for drug testing on human skin equivalents., Lab Chip. 15 (2015) 882–8. doi:10.1039/c4lc00999a.
[114] B. Ataç, I. Wagner, R. Horland, R. Lauster, U. Marx, A.G. Tonevitsky, et al., Skin and hair

on-a-chip: in vitro skin models versus ex vivo tissue maintenance with dynamic perfusion., Lab Chip. 13 (2013) 3555–61. doi:10.1039/c3lc50227a.
[115] K.H. Benam, R. Villenave, C. Lucchesi, A. Varone, C. Hubeau, H.-H. Lee, et al., Small airway-on-a-chip enables analysis of human lung inflammation and drug responses in vitro, Nat. Methods. (2015). doi:10.1038/nmeth.3697.
[116] A.T. O'Neill, N.A. Monteiro-Riviere, G.M. Walker, Characterization of microfluidic human epidermal keratinocyte culture, Cytotechnology. 56 (2008) 197–207. doi:10.1007/s10616-008-9149-9.
[117] L. Kim, M.D. Vahey, H.-Y. Lee, J. Voldman, Microfluidic arrays for logarithmically perfused embryonic stem cell culture, Lab Chip. 6 (2006) 394. doi:10.1039/b511718f.
[118] H. Lu, L.Y. Koo, W.M. Wang, D. a. Lauffenburger, L.G. Griffith, K.F. Jensen, Microfluidic shear devices for quantitative analysis of cell adhesion, Anal. Chem. 76 (2004) 5257–5264. doi:10.1021/ac049837t.
[119] I. Wagner, E.-M. Materne, S. Brincker, U. Süßbier, C. Frädrich, M. Busek, et al., A dynamic multi-organ-chip for long-term cultivation and substance testing proven by 3D human liver and skin tissue co-culture, Lab Chip. 13 (2013) 3538. doi:10.1039/c3lc50234a.
[120] I. Maschmeyer, A.K. Lorenz, K. Schimek, T. Hasenberg, A.P. Ramme, J. Hübner, et al., A four-organ-chip for interconnected long-term co-culture of human intestine, liver, skin and kidney equivalents, Lab Chip. 15 (2015) 2688–2699. doi:10.1039/C5LC00392J.
[121] I. Maschmeyer, T. Hasenberg, A. Jaenicke, M. Lindner, A.K. Lorenz, J. Zech, et al., Chip-based human liver-intestine and liver-skin co-cultures - A first step toward systemic repeated dose substance testing in vitro., Eur. J. Pharm. Biopharm. 95 (2015) 77–87. doi:10.1016/j.ejpb.2015.03.002.
[122] Y.-S. Sun, S.-W. Peng, J.-Y. Cheng, In vitro electrical-stimulated wound-healing chip for studying electric field-assisted wound-healing process., Biomicrofluidics. 6 (2012) 34117. doi:10.1063/1.4750486.
[123] I. Wagner, B. Atac, G. Lindner, R. Horland, M. Busek, F. Sonntag, et al., Skin and hair-on-a-chip: Hair and skin assembly versus native skin maintenance in a chip-based perfusion system, BMC Proc. 7 (2013) P93. doi:10.1186/1753-6561-7-S6-P93.
[124] N.S. Bhise, V. Manoharan, S. Massa, A. Tamayol, M. Ghaderi, M. Miscuglio, et al., A liver-on-a-chip platform with bioprinted hepatic spheroids, Biofabrication. 8 (2016) 14101. doi:10.1088/1758-5090/8/1/014101.
[125] S.J. Trietsch, G.D. Israëls, J. Joore, T. Hankemeier, P. Vulto, Microfluidic titer plate for stratified 3D cell culture., Lab Chip. 13 (2013) 3548–3554. doi:10.1039/c3lc50210d.
[126] K. Smeds, A. Pfister-Serres, D. Miki, K.A. Dastghieb, M. Inoue, D.L. Hatchell, et al., Novel Photocrosslinkable Polysaccharides for In Situ Hydrogel Formation, J. Biomed. Mat. Res. 54 (2001) 115–121.
[127] B. Duan, L.A. Hockaday, E. Kapetanovic, K.H. Kang, J.T. Butcher, Stiffness and adhesivity control aortic valve interstitial cell behavior within hyaluronic acid based hydrogels, Acta Biomater. 9 (2013) 7640–7650. doi:10.1016/j.actbio.2013.04.050.
[128] J.J. Rice, M.M. Martino, L. De Laporte, F. Tortelli, P.S. Briquez, J.A. Hubbell, Engineering the Regenerative Microenvironment with Biomaterials, Adv. Healthc. Mater. 2 (2013) 57–71. doi:10.1002/adhm.201200197.
[129] M. Xu, X., Jha, A, Harrington, DA., Farach-Carson, Hyaluronic Acid - Based Hydrogel: from a Natural Polysaccharide to Complex Networks, Soft Matter. 8 (2012) 3280–3294. doi:10.1039/C2SM06463D.Hyaluronic.
[130] L. Juhlin, Hyaluronan in skin., J. Intern. Med. 242 (1997) 61–66. doi:10.1046/j.1365-2796.1997.00175.x.
[131] R.K. Reed, K. Lilja, T.C. Laurent, Hyaluronan in the rat with special reference to the skin., Acta Physiol. Scand. 134 (1988) 405–411. doi:10.1111/j.1748-1716.1988.tb08508.x.
[132] Y.-H. Liao, S. a Jones, B. Forbes, G.P. Martin, M.B. Brown, Hyaluronan: pharmaceutical

characterization and drug delivery., Drug Deliv. 12 (2005) 327–342. doi:10.1080/10717540590952555.
[133] A. Aruffo, I. Stamenkovic, M. Melnick, C.B. Underhill, B. Seed, CD44 is the principal cell surface receptor for hyaluronate, Cell. 61 (1990) 1303–1313. doi:10.1016/0092-8674(90)90694-A.
[134] B. Widner, S. Von Dollen, M. Tang, T. Heu, A. Sloma, D. Sternberg, et al., Hyaluronic Acid Production in Bacillus subtilis, Appl. Environ. Microbiol. 71 (2005) 3747–3752. doi:10.1128/AEM.71.7.3747.
[135] A. Skardal, J. Zhang, L. McCoard, X. Xu, S. Oottamasathien, G.D. Prestwich, Photocrosslinkable Hyaluronan-Gelatin Hydrogels for Two-Step Bioprinting, Tissue Eng. Part A. 16 (2010) 2675–2685. doi:10.1089/ten.tea.2009.0798.
[136] B.R. Thakur, R.K. Singh, A.K. Handa, M.A. Rao, Chemistry and uses of pectin — A review, Crit. Rev. Food Sci. Nutr. 37 (1997) 47–73. doi:10.1080/10408399709527767.
[137] I. Braccini, S. Pérez, Molecular basis of Ca2+-induced gelation in alginates and pectins: The egg-box model revisited, Biomacromolecules. 2 (2001) 1089–1096. doi:10.1021/bm010008g.
[138] S.C. Neves, D.B. Gomes, A. Sousa, S.J. Bidarra, P. Petrini, L. Moroni, et al., Biofunctionalized pectin hydrogels as 3D cellular microenvironments, J. Mater. Chem. B. 3 (2015) 2096–2108. doi:10.1039/C4TB00885E.
[139] T.W. Wong, H.Y. Lee, L.W. Chan, P.W.S. Heng, Drug release properties of pectinate microspheres prepared by emulsification method, Int. J. Pharm. 242 (2002) 233–237. doi:10.1016/S0378-5173(02)00163-1.
[140] J.A. Burdick, G.D. Prestwich, Hyaluronic acid hydrogels for biomedical applications, Adv. Mater. 23 (2011) 41–56. doi:10.1002/adma.201003963.
[141] L. Möller, A. Krause, J. Dahlmann, I. Gruh, A. Kirschning, G. Dr??ger, Preparation and evaluation of hydrogel-composites from methacrylated hyaluronic acid, alginate, and gelatin for tissue engineering, Int. J. Artif. Organs. 34 (2011) 93–102. doi:10.5301/IJAO.2011.6397.
[142] D.F. Coutinho, S. V. Sant, H. Shin, J.T. Oliveira, M.E. Gomes, N.M. Neves, et al., Modified Gellan Gum hydrogels with tunable physical and mechanical properties, Biomaterials. 31 (2010) 7494–7502. doi:10.1016/j.biomaterials.2010.06.035.
[143] J. a Burdick, C. Chung, X. Jia, M. a Randolph, R. Langer, Controlled Degradation and Mechanical Behavior of Photopolymerized Hyaluronic Acid Networks Controlled Degradation and Mechanical Behavior of Photopolymerized Hyaluronic Acid Networks, Society. (2005) 386–391. doi:10.1021/bm049508a.
[144] K. Bott, Z. Upton, K. Schrobback, M. Ehrbar, J.A. Hubbell, M.P. Lutolf, et al., The effect of matrix characteristics on fibroblast proliferation in 3D gels, Biomaterials. 31 (2010) 8454–8464. doi:10.1016/j.biomaterials.2010.07.046.
[145] C. Branco da Cunha, D.D. Klumpers, W.A. Li, S.T. Koshy, J.C. Weaver, O. Chaudhuri, et al., Influence of the stiffness of three-dimensional alginate/collagen-I interpenetrating networks on fibroblast biology, Biomaterials. 35 (2014) 8927–8936. doi:10.1016/j.biomaterials.2014.06.047.
[146] F.R. Maia, K.B. Fonseca, G. Rodrigues, P.L. Granja, C.C. Barrias, Matrix-driven formation of mesenchymal stem cell-extracellular matrix microtissues on soft alginate hydrogels, Acta Biomater. 10 (2014) 3197–3208. doi:10.1016/j.actbio.2014.02.049.
[147] D. Lootens, F. Capel, D. Durand, T. Nicolai, P. Boulenguer, V. Langendorff, Influence of pH, Ca concentration, temperature and amidation on the gelation of low methoxyl pectin, Food Hydrocoll. 17 (2003) 237–244. doi:10.1016/S0268-005X(02)00056-5.
[148] S.A. Bencherif, A. Srinivasan, F. Horkay, J.O. Hollinger, K. Matyjaszewski, N.R. Washburn, Influence of the degree of methacrylation on hyaluronic acid hydrogels properties, Biomaterials. 29 (2008) 1739–1749. doi:10.1016/j.biomaterials.2007.11.047.
[149] D. a Gibbs, E.W. Merrill, K. a Smith, E. a Balazs, Rheology of hyaluronic acid.,

Biopolymers. 6 (1968) 777–791. doi:10.1002/bip.1968.360060603.
[150] F. Munarin, P. Petrini, M.C. Tanzi, M. a. Barbosa, P.L. Granja, Biofunctional chemically modified pectin for cell delivery, Soft Matter. 8 (2012) 4731. doi:10.1039/c2sm07260b.
[151] C.D. Pritchard, T.M. O'Shea, D.J. Siegwart, E. Calo, D.G. Anderson, F.M. Reynolds, et al., An injectable thiol-acrylate poly(ethylene glycol) hydrogel for sustained release of methylprednisolone sodium succinate, Biomaterials. 32 (2011) 587–597. doi:10.1016/j.biomaterials.2010.08.106.
[152] M.P. Lutolf, J. a Hubbell, Synthesis and Physicochemical Characterization of End-Linked Poly (ethylene glycol) -co-peptide Hydrogels Formed by Michael-Type Addition, Biomacromolecules. 4 (2003) 713–722. doi:10.1021/bm025744e.
[153] S.J. Bidarra, C.C. Barrias, K.B. Fonseca, M. a. Barbosa, R. a. Soares, P.L. Granja, Injectable in situ crosslinkable RGD-modified alginate matrix for endothelial cells delivery, Biomaterials. 32 (2011) 7897–7904. doi:10.1016/j.biomaterials.2011.07.013.
[154] J.R. Glass, K.T. Dickerson, K. Stecker, J.W. Polarek, Characterization of a hyaluronic acid-Arg-Gly-Asp peptide cell attachment matrix, Biomaterials. 17 (1996) 1101–1108. doi:10.1016/0142-9612(96)85911-4.
[155] F.Z. Cui, W.M. Tian, S.P. Hou, Q.Y. Xu, I.S. Lee, Hyaluronic acid hydrogel immobilized with RGD peptides for brain tissue engineering, J. Mater. Sci. Mater. Med. 17 (2006) 1393–1401. doi:10.1007/s10856-006-0615-7.
[156] Y. Lei, S. Gojgini, J. Lam, T. Segura, The spreading, migration and proliferation of mouse mesenchymal stem cells cultured inside hyaluronic acid hydrogels, Biomaterials. 32 (2011) 39–47. doi:10.1016/j.biomaterials.2010.08.103.
[157] G.-Z. Li, R. Randev, A.H. Soeriyadi, G.J. Rees, C. Boyer, Z. Tong, et al., Investigation into thiol-(meth)acrylate Michael addition reactions using amine and phosphine catalysts, Polym. Chem. 1 (2010) 1196–1204. doi:10.1039/c0py00100g.
[158] S.C. Rizzi, M. Ehrbar, S. Halstenberg, G.P. Raeber, H.G. Schmoekel, H. Hagenm??ller, et al., Recombinant protein-co-PEG networks as cell-adhesive and proteolytically degradable hydrogel matrixes. Part II: Biofunctional characteristics, Biomacromolecules. 7 (2006) 3019–3029. doi:10.1021/bm060504a.
[159] M.P. Lutolf, N. Tirelli, S. Cerritelli, L. Cavalli, J.A. Hubbell, Systematic modulation of Michael-type reactivity of thiols through the use of charged amino acids, Bioconjug. Chem. 12 (2001) 1051–1056. doi:10.1021/bc015519e.
[160] C.A. DeForest, B.D. Polizzotti, K.S. Anseth, Sequential click reactions for synthesizing and patterning three-dimensional cell microenvironments, Nat Mater. 8 (2009) 659–664. doi:10.1038/nmat2473.
[161] C. Zhang, S. Hekmatfer, N.W. Karuri, A comparative study of polyethylene glycol hydrogels derivatized with the RGD peptide and the cell-binding domain of fibronectin, J. Biomed. Mater. Res. - Part A. 102 (2014) 170–179. doi:10.1002/jbm.a.34687.
[162] Y.D. Park, N. Tirelli, J.A. Hubbell, Photopolymerized hyaluronic acid-based hydrogels and interpenetrating networks, Biomater. Silver Jubil. Compend. 24 (2006) 203–210. doi:10.1016/B978-008045154-1.50023-X.
[163] M. Zhou, A.M. Smith, A.K. Das, N.W. Hodson, R.F. Collins, R. V. Ulijn, et al., Self-assembled peptide-based hydrogels as scaffolds for anchorage-dependent cells, Biomaterials. 30 (2009) 2523–2530. doi:10.1016/j.biomaterials.2009.01.010.
[164] E. Ruoslahti, Rgd and Other Recognition Sequences for Integrins, Annu. Rev. Cell Dev. Biol. 12 (1996) 697–715. doi:10.1146/annurev.cellbio.12.1.697.
[165] E. Ruoslahti, M.D. Pierschbacher, New perspectives in cell adhesion: RGD and integrins., Science. 238 (1987) 491–497. doi:10.1126/science.2821619.
[166] D.E. Discher, Tissue Cells Feel and Respon to the Stiffness of Their Substrate, Science (80-.). 310 (2005) 1139–1143. doi:10.1126/science.1116995.
[167] K. Feld, Initial Adhesion of Human Fibroblasts in Serum-Free Medium : Possible Role of Secreted Fibronectin, 17 (1979) 117–129.

[168] J.A. Burdick, K.S. Anseth, Photoencapsulation of osteoblasts in injectable RGD-modified PEG hydrogels for bone tissue engineering, Biomaterials. 23 (2002) 4315–4323. doi:10.1016/S0142-9612(02)00176-X.
[169] G. Maheshwari, G. Brown, D. a Lauffenburger, a Wells, L.G. Griffith, Cell adhesion and motility depend on nanoscale RGD clustering., J. Cell Sci. 113 (Pt 1 (2000) 1677–1686. doi:10.1083/jcb.144.5.1019.
[170] M.P. Lutolf, J. a Hubbell, Synthetic biomaterials as instructive extracellular microenvironments for morphogenesis in tissue engineering., Nat. Biotechnol. 23 (2005) 47–55. doi:10.1038/nbt1055.